*Geol. Mag.* **141** (5), 2004, pp. 583–603. © 2004 Cambridge University Press
DOI: 10.1017/S0016756804009458 *Printed in the United Kingdom*


# Oceanic crust generation in an island arc tectonic setting, SE Anatolian orogenic belt (Turkey)

OSMAN PARLAK*, VOLKER HÖCK†, HÜSEYİN KOZLU‡ & MICHEL DELALOYE§

*Çukurova Üniversitesi, Jeoloji Mühendisliği Bölümü, 01330 Balcalı, Adana, Turkey
†University of Salzburg, Department of Geology & Paleontology, A-5020 Salzburg, Austria
‡Türkiye Petrolleri Anonim Ortaklığı, 06520 Ankara, Turkey
§University of Geneva, Department of Mineralogy, 1211 Geneva 4, Switzerland

(*Received* 19 May 2003; *revised version received* 15 March 2004; *accepted* 15 April 2004)

**Abstract** – A number of Late Cretaceous ophiolitic bodies are located between the metamorphic massifs of the southeast Anatolian orogenic system. One of them, the Göksun ophiolite (northern Kahramanmaraş), which crops out in a tectonic window bounded by the Malatya metamorphic units on both the north and south, is located in the EW-trending nappe zone of the southeast Anatolian orogenic belt between Göksun and Afşin (northern Kahramanmaraş). It consists of ultramafic–mafic cumulates, isotropic gabbro, a sheeted dyke complex, plagiogranite, volcanic rocks and associated volcanosedimentary units. The ophiolitic rocks and the tectonically overlying Malatya–Keban metamorphic units were intruded by syn-collisional granitoids (~85 Ma). The volcanic units are characterized by a wide spectrum of rocks ranging in composition from basalt to rhyolite. The sheeted dykes consist of diabase and microdiorite, whereas the isotropic gabbros consist of gabbro, diorite and quartzdiorite. The magmatic rocks in the Göksun ophiolite are part of a co-magmatic differentiated series of subalkaline tholeiites. Selective enrichment of some LIL elements (Rb, Ba, K, Sr and Th) and depletion of the HFS elements (Nb, Ta, Ti, Zr) relative to N-MORB are the main features of the upper crustal rocks. The presence of negative anomalies for Ta, Nb, Ti, the ratios of selected trace elements (Nb/Th, Th/Yb, Ta/Yb) and normalized REE patterns all are indicative of a subduction-related environment. All the geochemical evidence both from the volcanic rocks and the deeper levels (sheeted dykes and isotropic gabbro) show that the Göksun ophiolite formed during the mature stage of a suprasubduction zone (SSZ) tectonic setting in the southern branch of the Neotethyan ocean between the Malatya–Keban platform to the north and the Arabian platform to the south during Late Cretaceous times. Geological, geochronological and petrological data on the Göksun ophiolite and the Baskil magmatic arc suggest that there were two subduction zones, the first one dipping beneath the Malatya–Keban platform, generating the Baskil magmatic arc and the second one further south within the ocean basin, generating the Göksun ophiolite in a suprasubduction zone environment.

Keywords: Göksun ophiolite, geochemistry, Turkey, subduction zones, Neotethys.

## 1. Introduction

Late Cretaceous ophiolites in Turkey are located in five main zones. From north to south these are (1) Pontide ophiolites, (2) Anatolian ophiolite belt, (3) Tauride ophiolite belt, (4) Southeast Anatolian ophiolites and (5) the peri-Arabian platform ophiolites (Fig. 1) (Robertson, 2002). The main characteristics of the Pontide ophiolite belt is the presence of ensimatic island arc and ophiolitic units (Ustaömer & Robertson, 1997). The central Anatolia are characterized by three different groups, namely (1) ophiolites located on the Kırşehir and Nigde metamorphic massifs, (2) Ankara mélange and (3) metamorphosed ophiolites in the Izmir–Ankara suture to the north of the Menderes massif (Yalınız, Floyd & Göncüoğlu, 1996, 2000; Robertson, 2002). The Tauride ophiolites start with the Lycian nappes to the west and end with the Pınarbaşı ophiolite to the east. These ophiolites are situated either on the northern or southern flank of the EW-trending Tauride carbonate platform axis (Juteau, 1980; Dilek & Moores, 1990; Dilek *et al*. 1999; Parlak, Delaloye & Bingöl, 1996; Parlak, Höck & Delaloye, 2000, 2002). The southeast Anatolian ophiolite belt, the only one considered in this paper, is characterized, from west to east, by the Göksun, İspendere, Guleman and Yüksekova ophiolites and their metamorphosed equivalents such as the Kömürhan and Berit metaophiolites (Yazgan & Chessex, 1991; Yılmaz, 1993; Yılmaz, Yiğitbaş & Genç, 1993; Beyarslan & Bingöl, 2000; Robertson, 2002).

The Late Cretaceous ophiolites in the eastern Mediterranean region show three distinct tectonic environments for their genesis. These are (1) mid-ocean ridge type (MOR) (Shallo, Kodra & Gjata, 1990; Bortolotti *et al*. 1996; Jones, Robertson & Cann, 1991; Smith *et al*. 1975); (2) transitional between MOR and subduction-related (Höck *et al*. 2002; Koepke,

* Author for correspondence: parlak@cukurova.edu.tr

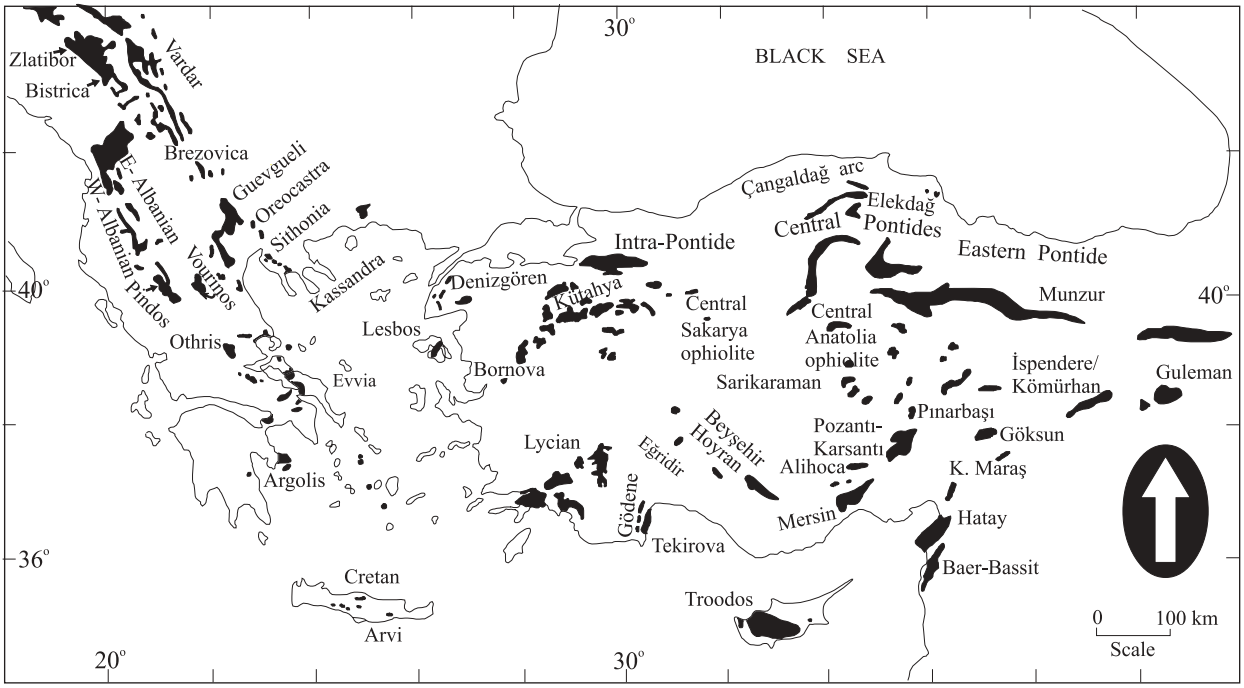


Figure 1. Distribution of the Neotethyan ophiolites in the eastern Mediterranean region (after Robertson, 2002).

Seidel & Kreuzer, 2002; Capedri *et al*. 1980; Jones, Robertson & Cann, 1991; Pamic, Tomljenovic & Balen, 2002); and (3) subduction-related (Beccaluva *et al*. 1994; Robertson & Shallo, 2000; Rassios *et al*. 1983; Beccaluva *et al*. 1994; Parlak, Delaloye & Bingöl, 1996; Yalınız, Floyd & Göncüoğlu, 1996; Parlak, Höck & Delaloye, 2000; Thy, 1987; Hébert & Laurent, 1990; Al-Riyami *et al*. 2002).

Recently, Shervais (2001) reviewed subduction-related ophiolites and proposed an evolutionary scenario that consists of five stages, overlapping with each other in time and space, named according to the biological life cycle: birth, youth, maturity, death and resurrection stages. Although there are number of ophiolites that possess all the characteristics of the suprasubduction life cycle such as Oman, Vourinos in Greece, the Coast Range in California, the Bay of Islands in Newfoundland (Shervais, 2001, and references therein), the main features of suprasubduction zone ophiolites are generally formed during the first two stages (birth and youth); they never reach maturity but skip directly to death and resurrection (Shervais, 2001).

The well-documented ophiolites along the Taurides and the Peri-Arabic belt in southern Turkey were generally formed during the first two stages (birth and youth) of the suprasubduction zone life cycle. The Mersin (Parlak, Delaloye & Bingöl, 1995, 1996) and Pozantı–Karsantı (Lytwyn & Casey, 1995; Dilek *et al*. 1999; Parlak, Höck & Delaloye, 2000, 2002) ophiolites from the Tauride belt in southern Turkey are good candidates for the birth stage, characterized by the presence of low-K tholeiitic lavas and well-developed gabbroic cumulates, whereas the Hatay (Kızıldağ) ophiolite from the Arabian border in southern Turkey (Dilek & Delaloye, 1992; Dilek & Thy, 1998) is a good example of the youth stage, characterized by the low-K tholeiites (Lytwyn & Casey, 1993), boninites (Dubertret, 1955), ductilely deformed layered gabbro and wehrlitic xenoliths in gabbroic cumulates.

The aim of this paper is to present, for the first time, detailed geochemical work on the volcanic and plutonic components of one of the most complete and best exposed mature stage ophiolites (*sensu* Shervais, 2001) in the eastern Mediterranean region, and to show how the results can be interpreted in terms of spatial and temporal relations between the Göksun ophiolite and the Andean-type Baskil magmatic arc in southeastern Turkey during the Late Cretaceous period.

## 2. Regional geology

Anatolia consists of a number of microcontinents or blocks separated by suture zones of various ages. The Anatolian orogen is subdivided into EW-trending belts from north to south, namely Pontides, Sakarya continent, Anatolides–Taurides and Southeast Anatolian Border Folds (Şengör & Yılmaz, 1981). The Tethyan evolution of Anatolia is represented by two main stages of tectonic activity: the Palaeotethyan and Neotethyan events. The Palaeotethyan events, between the Permian and the Liassic, operated mainly in northern Anatolia (Ustaömer & Robertson, 1997), whereas the Neotethyan events were effective throughout Anatolia between Triassic and Miocene times (Şengör & Yılmaz, 1981; Robertson & Dixon, 1984).

https://doi.org/10.1017/S0016756804009458 Published online by Cambridge University Press

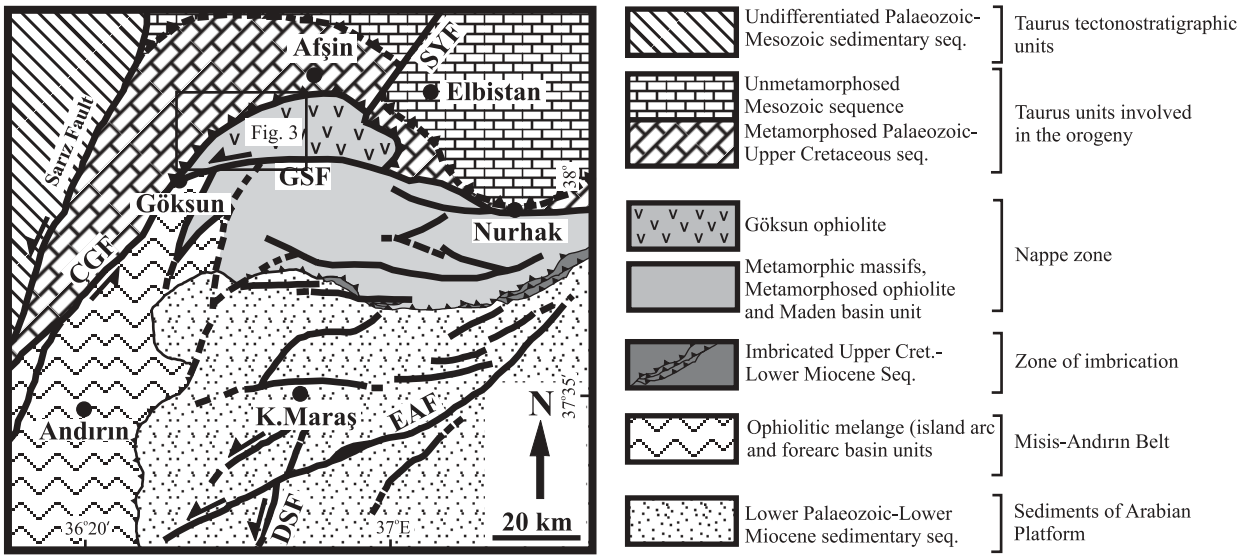


Figure 2. Tectonic units and structural features of the Kahramanmaras–Elbistan regions (simplified from Yılmaz, 1993). Location of Figure 3 is also shown. Key to the abbreviations: EAF – East Anatolian Fault, DSF – Dead Sea Fault, ÇGF – Çiçekli–Göksun Fault, GSF – Göksun–Sürgü Fault, SYF – Sarıyatak Fault.

The southeast Anatolian orogenic segment comprises three distinct, approximately EW-trending, tectonic elements which are separated from one another by major N-dipping thrust faults (Fig. 2). From north to south, these are the nappe zone, the zone of imbrication and the Arabian platform (Yılmaz, 1990, 1993; Yılmaz, Yiğitbaş & Genç, 1993). The nappe zone in the southeast Anatolian orogen forms, morphologically, the highest tectonic unit, which consists of two large nappe stacks, the lower and the upper nappes (Yılmaz, 1993). The lower nappe is mainly characterized by variably metamorphosed Cretaceous ophiolitic units (e.g. Kızılkaya, Berit and Yüksekova) and the Maden Group which contains a volcanic and sedimentary rock sequence of Middle Eocene age possibly representing a short-lived back-arc basin (Yılmaz, Yiğitbaş & Genç, 1993; Yiğitbaş & Yılmaz, 1996) or pull-apart basin (Aktaş & Robertson, 1984). The upper nappe, ranging in age from from Palaeozoic to Campanian, is represented by the metamorphic massifs (Bitlis, Pütürge, Malatya, Keban, Engizek and Binboğa) of southeast Anatolia (Ketin, 1983; Yılmaz, 1993). Yılmaz & Yiğitbaş (1991) suggested that, because of their similarity in terms of age, lithology and metamorphism, these bodies were part of a tectono-stratigraphic unit that was disrupted and fragmented during the orogeny. Yılmaz *et al*. (1987) assumed that the metamorphism was related to the ophiolite obduction and occurred during the Campanian to early Maastrichtian time interval. The imbrication zone is a narrow EW-trending belt which was squeezed between the nappe region to the north and the Arabian platform to the south (Fig. 2). The zone of imbrication is represented by a number of N-dipping thrust slices with southerly vergence (Yılmaz *et al*. 1987; Yılmaz, 1990; Karig & Kozlu, 1990; Aktaş & Robertson, 1984). The rock units in the imbricated thrust sheets range in age from Late Cretaceous to Early Miocene (Yılmaz, 1993). The rock units in the imbrication zone appear to be the lateral, but more distal, equivalents of the Arabian platform units, distal either towards the northerly situated continental slope and the abyssal plain (Yılmaz *et al*. 1987). The Arabian platform comprises autochthonous and parautochthonous sedimentary units deposited since Early Palaeozoic time (Fig. 2) as well as Upper Cretaceous ophiolite nappes and their sedimentary cover (Yılmaz, 1990).

The Late Cretaceous Göksun ophiolite, tectonically bounded by the Malatya metamorphic units on the north and south, is located in the EW-trending nappe zone of the southeast Anatolian orogenic belt in the area between Göksun and Afşin (Kahramanmaraş) (Fig. 3). The repetition of the Malatya metamorphic massif seems to be due to S-directed tectonic imbrication as a result of thrust faulting and left lateral strike-slip faulting associated with the East Anatolian fault zone (Fig. 3). Mantle tectonites at the base of the ophiolite in the Göksun–Afşin (Kahramanmaraş) area were obliterated as a result of nappe emplacement during the Late Cretaceous (Figs 3, 4). The ophiolitic rocks and the tectonically overlying Malatya metamorphic rocks were intruded by a syn-collisional granitoids (Figs 3, 4). The oceanic crustal section of the Göksun ophiolite starts with the ultramafic and mafic cumulates which crop out mainly in the middle of the study area between Fındık and Domuzdere (Figs 3, 4). A small outcrop of the cumulates is seen to the west of Yazıköy (Fig. 3). These rocks display cumulate structures such as igneous lamination and rhythmic layering. The contact with the isotropic gabbro is tectonic. Isotropic gabbros

https://doi.org/10.1017/S0016756804009458 Published online by Cambridge University Press

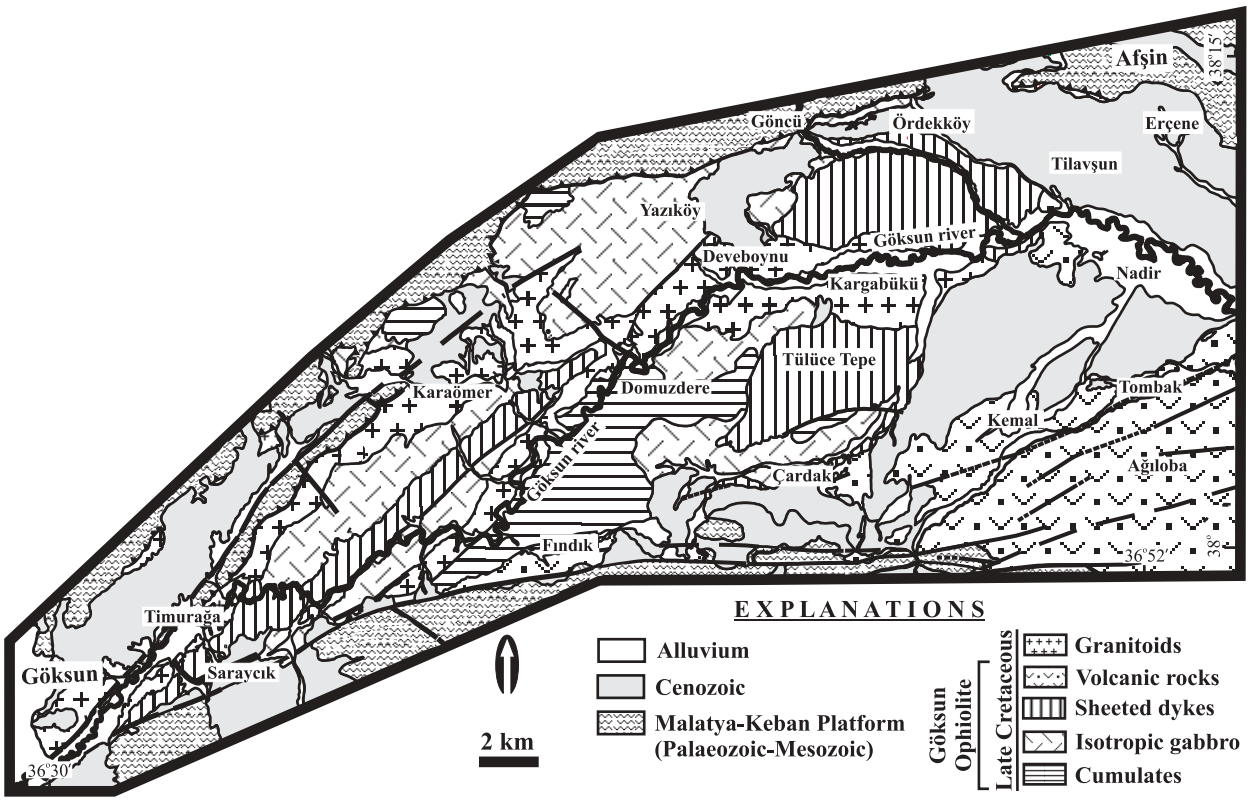


Figure 3. Geological map of the Göksun ophiolite in the area between Göksun and Afşin (Kahramanmaraş), southeastern Turkey (modified from Perinçek & Kozlu, 1984).

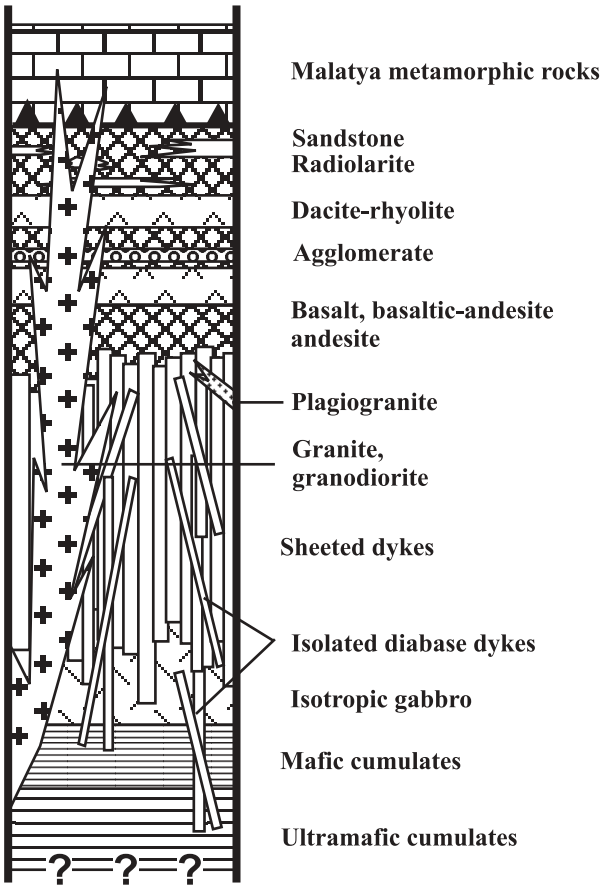


Figure 4. Synthetic log of the Göksun ophiolite.

are observed in different parts of the study area, namely in Yazıköy, southwest of Karaömer, north of Çardak and Domuzdere. Isotropic gabbros gradually pass into sheeted dyke rocks between Domuzdere and Tülüce Tepe (Fig. 3). Here, isolated dyke intrusions appear in the upper part of the isotropic gabbros, and these dykes become dominant in the lower part of the sheeted dykes, separated by small gabbro screens. Dyke thicknesses range from 10 cm to 1 m. Small intrusive bodies of plagiogranite are observed in the sheeted dyke complex (Fig. 4). The volcanic section mainly crops out in the east around Çardak, Kemal, Tombak and Ağıloba (Fig. 3), although contact relationships with the underlying units are obscured by Cenozoic units (Fig. 3). The basic volcanic rocks crop out as pillow lavas and massive lavas, whereas the acidic volcanic rocks form lava flows. Sedimentary units covering the volcanic section comprise volcanogenic sandstone, tuff, agglomerate, mudstone and limestone (Fig. 4). Perinçek & Kozlu (1984) dated the cover sediments of the volcanic rocks as Upper Cretaceous.

The evolution of the southeast Anatolian orogenic system caused the progressive movement of nappes toward the Arabian plate during Late Cretaceous–Miocene times (Yılmaz, 1993). The initial emplacement of the Göksun ophiolite over the Arabian platform was during Late Cretaceous times (Perinçek & Kozlu, 1984; Yılmaz, 1993). The Malatya–Keban platform rocks were thrust over the ophiolitic units during the Late Cretaceous. The Göksun ophiolite and the

https://doi.org/10.1017/S0016756804009458 Published online by Cambridge University Press

Malatya–Keban platform were later thrust over the Maden group during the Late Eocene (Perinçek & Kozlu, 1984; Yılmaz, 1993) as a result of progressive elimination of the ocean and southerly movement of the nappes in the region.

## 3. Petrography

The Göksun ophiolite comprises, in ascending order: ultramafic to mafic cumulates; isotropic gabbros; a sheeted dyke complex, volcanic rocks and associated sedimentary rock units (Fig. 4). The ultramafic (wehrlite and lherzolite) cumulates display mesocumulate and poikilitic texture. The wehrlite is dominated by olivine (65–70 %), clinopyroxene (20–25 %), orthopyroxene (<5 %) and plagioclase (<1 %). The pyroxenes are partly transformed to amphibole. Plagioclase is partly altered to sericite and kaolinite. The lherzolite consists of olivine (70 %), orthopyroxene (15–20 %) and clinopyroxene (15–20 %) with rare chromite crystals set in variably serpentinized olivine and pyroxene.

Mafic cumulate rocks (olivine gabbro and gabbro) display ortho- and mesocumulate textures. The olivine-gabbro is dominated by plagioclase (labradorite) (65–70 %), clinopyroxene (15 %) and olivine (10 %). Fe–Ti oxide (magnetite) occurs within the cracked olivines as a result of serpentinization. Prehnite and kaolinite are seen as secondary products of plagioclases. The gabbroic cumulates consist of plagioclase (65–70 %) and clinopyroxene (25–30 %). Chromite crystals are present as accessory phases, and the clinopyroxenes are partly transformed to amphibole.

Isotropic plutonic rocks in the Göksun ophiolite include gabbro, diorite and quartz-diorite. Gabbros display a non-cumulus granular to poikilitic texture and are characterized by primary plagioclase ($An_{59-60}$), pyroxene and secondary amphibole, and are often associated with secondary calcite, zeolite, actinolite and opaque (Fe–Ti oxide) minerals. Diorites display granular to micrographic texture, and are characterized by primary and secondary plagioclase, hornblende and pyroxene. The micrographic texture in diorites is thought to be the consequence of secondary albite generation within the primary plagioclases ($An_{30-35}$). Granular to micrographic quartz diorites are dominated by plagioclase (65–70 %), pyroxene (20–25 %), and xenomorphic quartz (10 %). Sphene and opaque Fe–Ti oxides are accessory phases, whereas actinolite, epidote, zeolite, chlorite and quartz are secondary phases in the rocks.

The Göksun ophiolite sheeted dyke complex shows primary contact relationships with the isotropic gabbro at its base. The complex starts with isolated dykes at the basal contact with the isotropic gabbro, and is dominated by 100 % dykes ranging in thickness from 10 cm to 1 m in the upper levels. The dykes root into the gabbro, suggesting their derivation from the isotropic gabbro. The isolated dykes and the sheeted dykes show the same petrographical and geochemical features, and are characterized by diabase and microdiorite. The diabase, displaying intersertal texture, is represented by a greenschist facies assemblage consisting of secondary plagioclase, chlorite, epidote and opaque minerals. The microdiorite, displaying microgranular texture, is characterized by plagioclase ($An_{40-50}$), amphibole, and opaque Fe–Ti oxides.

Volcanic rocks in the Göksun ophiolite are represented by a wide spectrum of rocks including basalt, basaltic andesite, andesite, dacite and rhyolite. Mafic to intermediate volcanic rocks of the Göksun ophiolite crop out as pillow and massive lavas, whereas the acidic members are observed as lava flows intercalated with the pillows. The volcanic rocks are interbedded with volcaniclastic material, volcanogenic sandstone, tuff and pelagic limestone at different levels. The basalts display aphanitic, microlitic to microlitic porphyric textures and are dominated by plagioclase and pyroxene phyric lavas. The basaltic andesites show intersertal, microlitic to microlitic porphyric texture. They are plagioclase phyric and contain subordinate subhedral clinopyroxene as phenocryst phases. The andesitic lavas display intersertal, amygdaloidal and porphyric texture. They are plagioclase phyric andesites. The proportion of quartz is increased within the andesitic volcanic rocks. The dacites, displaying porphyric texture, are plagioclase phyric lavas. The plagioclase is seen either as phenocrysts or as microliths within the matrix. Quartz is observed as phenocrysts in the rock. The rhyolitic volcanic rocks show porphyritic texture and are characterized by corroded quartz and plagioclase phenocrysts set in a groundmass that is composed of fine-grained plagioclase and K-feldspar. The common secondary phases in the mafic and felsic volcanic rocks are epidote, chlorite, calcite, albite, quartz and kaolin.

Secondary phases (epidote, albite, chlorite, actinolite) reveal the effects of alteration within the Göksun ophiolite rock units. The dominant secondary assemblages point to a greenschist facies metamorphism. Moreover, quartz and carbonate phases occuring as veinlets show the effects of low-temperature fluids that circulated throughout the rock units.

## 4. Analytical methods

A total of 112 samples from the volcanic rocks (77), sheeted dykes (22) and isotropic gabbros (13) were analysed for major and trace elements by XRF in the Mineralogy Department at the University of Geneva. Major element contents were determined on glass beads fused from ignited powders to which $Li_2B_4O_7$ was added at a ratio of 1:5, in a gold–platinum crucible at 1150 °C. Trace element contents were measured by XRF on pressed-powder pellets. A subset of 17 representative samples (ten volcanic rocks, four sheeted dykes and three isotropic gabbros) were analysed by

https://doi.org/10.1017/S0016756804009458 Published online by Cambridge University Press

Table 1. Summary table for the geochemical features of the crustal rocks in the Göksun ophiolite

| Group | Rock type | $SiO_2$ (wt %) | $TiO_2$ (wt %) | $Na_2O + K_2O$ (wt %) | Zr (ppm) | Data |
|---|---|---|---|---|---|---|
| 1 | Basalt | 51.79–41.79 | 1.87–0.35 | 5.32–0.22 | 132–25 | Table 2 |
| 2 | Basaltic-andesite | 55.01–52.21 | 1.93–0.56 | 7.93–0 | 152–50 | Table 3 |
| 3 | Andesite | 61.67–55.74 | 2.03–0.58 | 9.77–0.27 | 159–42 | Table 4 |
| 4 | Dacite | 69.2–62.96 | 0.84–0.45 | 6.66–2.96 | 164–58 | Table 5 |
| 5 | Rhyolite | 77.19–75.75 | 0.24–0.23 | 5.52–5.46 | 139–136 | Table 5 |
| 6 | Sheeted dykes | 62.1–48.57 | 2.18–0.52 | 6.2–0.01 | 136–28 | Table 6 |
| 7 | Isotropic gabbro | 67.73–50.59 | 1.43–0.93 | 7.07–3.93 | 197–61 | Table 7 |

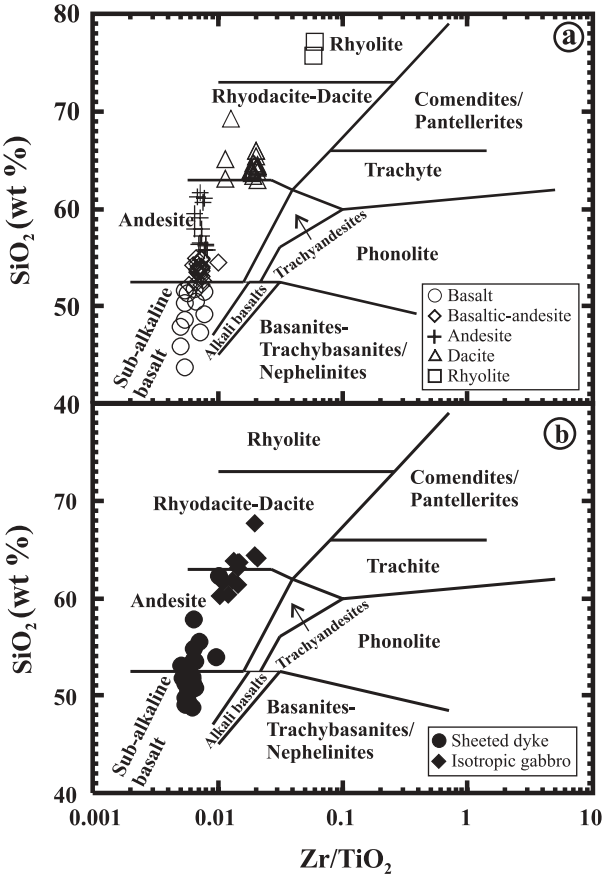


Figure 5. Discrimination of different rock types from the volcanic rocks (a), sheeted dykes and isotropic gabbros (b) of the Göksun ophiolite (after Floyd & Winchester, 1978).

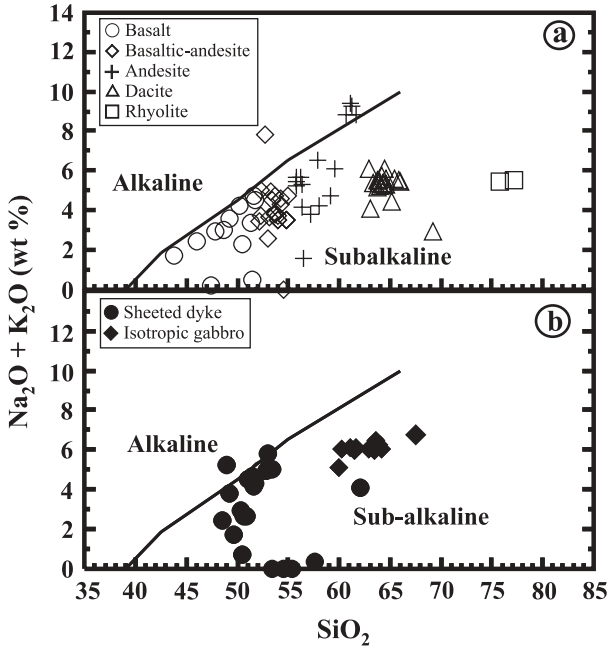


Figure 6. Alkali v. silica plots of the volcanic rocks (a), sheeted dykes and isotropic gabbros (b) from the Göksun ophiolite (after Irvine & Baragar, 1971).

ICP-MS for trace elements (including REE) at Actlabs-Activation Laboratories in Canada. The results of the analyses are presented in Tables 2 to 8.

## 5. Geochemistry

The extrusive rocks in the Göksun ophiolite are represented by five different lava units (basalt to rhyolite) based on their Zr/Ti ratios and silica ($SiO_2$) contents, illustrated in Figure 5a (Floyd & Winchester, 1978). The geochemical characteristics of each group are summarized in Table 1. The sheeted dyke rocks are characterized by diabase to microdiorite, whereas the isotropic gabbroic rocks are represented by diorite to quartz diorite based on their Zr/Ti ratios and silica ($SiO_2$) contents, shown in Figure 5b (Floyd & Winchester, 1978). The geochemical features of the sheeted dykes and isotropic gabbros are summarized in Table 1. The crustal rocks of the Göksun ophiolite are tholeiitic based on their total alkali-silica contents (Irvine & Baragar, 1971) (Fig. 6), and their low Nb/Y ratios (volcanic rocks (0.04–0.22), sheeted dykes (0.03–0.15) and isotropic gabbros (0.04–0.09)) (Winchester & Floyd, 1977) (Tables 2–8).

Selected incompatible trace elements, in particular Zr, Nb, Y, Ti and REE, have been shown to be the least mobile during alteration processes (Thompson, 1973; Pearce & Cann, 1973; Humphris & Thompson, 1978). These incompatible trace elements may be useful in characterizing petrological affinities and the past tectonic environment of volcanic rocks (Pearce & Cann, 1973; Floyd & Winchester, 1975; Pearce & Norry, 1979). Since the volcanic rocks, sheeted dykes and isotropic gabbros in the Göksun ophiolite show some low-grade secondary alteration, one can expect selected major and trace element (especially

https://doi.org/10.1017/S0016756804009458 Published online by Cambridge University Press

Table 2. Major and trace element analyses of basaltic volcanic rocks in the Göksun ophiolite, southeastern Turkey

| Sample | K-80 | K-81 | K-82 | K-83 | K-84 | K-89 | K-92 | K-93 | K-98 | K-118 | K-121 | K-124 | K-129 | K-212 | K-218 |
|---|---|---|---|---|---|---|---|---|---|---|---|---|---|---|---|
| $SiO_2$ | 48.62 | 45.96 | 47.85 | 41.76 | 50.86 | 46.54 | 51.58 | 51.79 | 50.48 | 50.27 | 51.37 | 51.49 | 49.23 | 47.36 | 43.76 |
| $TiO_2$ | 0.61 | 0.58 | 0.58 | 0.82 | 0.90 | 0.95 | 1.34 | 1.24 | 1.64 | 1.85 | 1.87 | 1.71 | 0.83 | 0.35 | 0.49 |
| $Al_2O_3$ | 14.98 | 15.39 | 14.23 | 13.17 | 16.50 | 15.93 | 15.02 | 15.39 | 13.57 | 14.94 | 14.80 | 14.95 | 16.02 | 13.81 | 12.97 |
| FeO* | 9.32 | 10.12 | 9.70 | 7.68 | 7.89 | 9.45 | 12.26 | 10.92 | 12.76 | 13.51 | 12.71 | 11.23 | 6.93 | 6.99 | 9.75 |
| MnO | 0.16 | 0.16 | 0.16 | 0.20 | 0.34 | 0.26 | 0.24 | 0.22 | 0.18 | 0.33 | 0.27 | 0.20 | 0.21 | 0.17 | 0.14 |
| MgO | 10.37 | 11.21 | 11.40 | 5.40 | 2.06 | 10.06 | 7.25 | 6.85 | 4.69 | 5.36 | 4.60 | 2.77 | 4.02 | 6.39 | 10.94 |
| CaO | 9.72 | 10.14 | 9.73 | 14.70 | 10.90 | 4.81 | 6.66 | 7.07 | 5.67 | 4.89 | 7.54 | 12.99 | 5.64 | 15.39 | 11.64 |
| $Na_2O$ | 2.69 | 1.91 | 2.77 | 3.26 | 4.75 | 3.99 | 4.56 | 4.40 | 2.19 | 4.21 | 3.22 | 0.53 | 3.10 | 0.22 | 1.27 |
| $K_2O$ | 0.34 | 0.57 | 0.20 | 0.07 | 0.14 | 0.02 | 0.20 | 0.16 | 0.11 | 0.06 | 0.13 | 0.01 | 0.47 | 0.00 | 0.43 |
| $P_2O_5$ | 0.06 | 0.05 | 0.05 | 0.11 | 0.15 | 0.08 | 0.12 | 0.13 | 0.15 | 0.20 | 0.19 | 0.27 | 0.11 | 0.05 | 0.04 |
| $Cr_2O_3$ | 0.11 | 0.12 | 0.12 | 0.05 | 0.05 | 0.05 | 0.02 | 0.02 | 0.00 | 0.03 | 0.05 | 0.04 | 0.04 | 0.10 | 0.16 |
| NiO | 0.03 | 0.03 | 0.03 | 0.02 | 0.01 | 0.01 | 0.01 | 0.01 | 0.00 | 0.01 | 0.02 | 0.01 | 0.02 | 0.04 | 0.05 |
| $CO_2$ | | | | 8.30 | 3.40 | 2.18 | | | | | | | | | |
| LOI | 3.50 | 4.05 | 3.51 | 2.74 | 1.47 | 5.50 | 1.02 | 2.17 | 8.79 | 4.57 | 2.77 | 3.67 | 13.81 | 9.18 | 8.48 |
| Total | 100.50 | 100.29 | 100.32 | 98.27 | 99.43 | 99.83 | 100.27 | 100.36 | 100.23 | 100.23 | 99.53 | 99.88 | 100.41 | 100.06 | 100.11 |
| Nb | 1 | 1 | 1 | 1 | 1 | 2 | 2 | 2 | 3 | 5 | 4 | 4 | 3 | 1 | 1 |
| Zr | 33 | 29 | 29 | 67 | 71 | 56 | 73 | 80 | 111 | 101 | 107 | 132 | 64 | 25 | 27 |
| Y | 20 | 19 | 19 | 23 | 25 | 29 | 29 | 32 | 30 | 33 | 34 | 36 | 24 | 13 | 15 |
| Sr | 137 | 108 | 124 | 127 | 162 | 85 | 152 | 163 | 53 | 169 | 178 | 346 | 256 | 37 | 54 |
| U | 2 | 2 | 2 | 2 | 2 | 2 | 2 | 2 | 2 | 2 | 3 | 2 | 2 | 2 | 2 |
| Rb | 8 | 13 | 6 | 2 | 1 | 2 | 3 | 2 | 1 | 4 | 5 | 2 | 10 | 2 | 11 |
| Th | 2 | 3 | 2 | 4 | 2 | 6 | 2 | 2 | 2 | 2 | 2 | 2 | 2 | 2 | 2 |
| Pb | 13 | 13 | 16 | 9 | 7 | 8 | 8 | 9 | 15 | 6 | 5 | 9 | 2 | 7 | 8 |
| Ga | 15 | 15 | 14 | 15 | 17 | 19 | 17 | 18 | 20 | 19 | 20 | 26 | 18 | 20 | 12 |
| Ni | 192 | 195 | 217 | 151 | 101 | 74 | 53 | 49 | 2 | 9 | 10 | 3 | 31 | 37 | 292 |
| Co | 51 | 53 | 58 | 40 | 34 | 46 | 36 | 38 | 46 | 46 | 39 | 27 | 26 | 27 | 61 |
| Cr | 890 | 1640 | 1429 | 1517 | 376 | 760 | 74 | 97 | 111 | 42 | 36 | 24 | 86 | 281 | 987 |
| V | 267 | 280 | 248 | 280 | 326 | 350 | 392 | 329 | 493 | 515 | 436 | 243 | 338 | 300 | 241 |
| Ba | 19 | 15 | 9 | 45 | 9 | 9 | 52 | 27 | 9 | 32 | 33 | 9 | 133 | 37 | 113 |
| Hf | 13 | 11 | 9 | 4 | 5 | 6 | 7 | 7 | 6 | 6 | 3 | 5 | 5 | 1 | 1 |
| Sc | 49 | 62 | 54 | 55 | 31 | 83 | 15 | 25 | 36 | 66 | 46 | 32 | 45 | 31 | 58 |
| Nb/Y | 0.05 | 0.05 | 0.05 | 0.04 | 0.04 | 0.07 | 0.07 | 0.06 | 0.10 | 0.15 | 0.12 | 0.11 | 0.13 | 0.08 | 0.07 |

Total Fe is expressed as FeO*. Major elements in wt %, trace elements in ppm.

Table 3. Major and trace element analyses of the basaltic andesite volcanic rocks in the Göksun ophiolite, southeastern Turkey

| Sample | K-86 | K-91 | K-94 | K-95 | K-97 | K-119 | K-120 | K-123 | K-125 | K-126 | K-127 | K-128 | K-130 | K-131 | K-132 | K-133 | K-134 | K-135 | K-136 | K-137 | K-213 | K-216 |
|---|---|---|---|---|---|---|---|---|---|---|---|---|---|---|---|---|---|---|---|---|---|---|
| $SiO_2$ | 55.01 | 52.25 | 52.34 | 52.60 | 53.32 | 53.64 | 54.90 | 53.45 | 54.30 | 53.03 | 52.21 | 53.16 | 53.76 | 53.98 | 54.76 | 54.00 | 53.68 | 54.04 | 54.88 | 54.25 | 52.68 | 54.56 |
| $TiO_2$ | 1.77 | 0.85 | 1.51 | 1.35 | 1.39 | 1.93 | 1.91 | 1.88 | 1.92 | 1.32 | 1.06 | 1.02 | 0.99 | 1.03 | 0.98 | 1.01 | 1.01 | 1.00 | 1.00 | 1.78 | 0.85 | 0.56 |
| $Al_2O_3$ | 14.60 | 14.55 | 15.37 | 15.12 | 15.45 | 15.13 | 14.88 | 14.45 | 14.82 | 14.26 | 18.62 | 18.31 | 18.28 | 18.26 | 17.61 | 17.79 | 18.14 | 18.12 | 17.77 | 14.89 | 18.03 | 14.03 |
| FeO* | 10.20 | 11.69 | 10.73 | 10.64 | 11.00 | 11.65 | 11.47 | 11.37 | 11.50 | 9.30 | 8.73 | 8.39 | 8.41 | 8.45 | 8.34 | 8.27 | 8.35 | 8.23 | 8.32 | 12.30 | 10.26 | 7.18 |
| MnO | 0.18 | 0.20 | 0.19 | 0.18 | 0.16 | 0.30 | 0.29 | 0.31 | 0.31 | 0.16 | 0.26 | 0.25 | 0.21 | 0.22 | 0.25 | 0.26 | 0.24 | 0.22 | 0.25 | 0.15 | 0.12 | 0.15 |
| MgO | 4.13 | 8.90 | 6.44 | 5.83 | 6.54 | 3.50 | 3.56 | 3.33 | 3.38 | 3.65 | 4.89 | 4.54 | 4.65 | 4.65 | 4.78 | 4.85 | 4.55 | 4.56 | 4.71 | 4.32 | 1.84 | 6.11 |
| CaO | 3.94 | 3.10 | 7.12 | 6.73 | 4.46 | 5.03 | 4.56 | 5.95 | 4.73 | 10.51 | 7.38 | 7.20 | 7.17 | 7.12 | 6.52 | 6.25 | 7.02 | 7.05 | 6.59 | 4.01 | 3.84 | 12.46 |
| $Na_2O$ | 5.34 | 3.71 | 4.72 | 5.07 | 4.83 | 4.63 | 4.64 | 4.39 | 4.48 | 2.57 | 3.06 | 3.31 | 3.45 | 3.11 | 3.15 | 3.12 | 3.41 | 3.36 | 3.15 | 4.26 | 6.52 | 0.00 |
| $K_2O$ | 0.02 | 0.02 | 0.31 | 0.30 | 0.12 | 0.09 | 0.08 | 0.13 | 0.13 | 0.01 | 0.36 | 0.36 | 0.40 | 0.39 | 0.36 | 0.39 | 0.37 | 0.39 | 0.39 | 0.06 | 1.31 | 0.00 |
| $P_2O_5$ | 0.24 | 0.08 | 0.17 | 0.13 | 0.15 | 0.20 | 0.20 | 0.20 | 0.21 | 0.13 | 0.15 | 0.15 | 0.14 | 0.15 | 0.14 | 0.14 | 0.14 | 0.14 | 0.15 | 0.16 | 0.11 | 0.09 |
| $Cr_2O_3$ | 0.00 | 0.04 | 0.01 | 0.01 | 0.00 | 0.05 | 0.01 | 0.06 | 0.02 | 0.01 | 0.03 | 0.01 | 0.03 | 0.06 | 0.06 | 0.06 | 0.04 | 0.04 | 0.06 | 0.04 | 0.11 | 0.09 |
| NiO | 0.00 | 0.01 | 0.00 | 0.00 | 0.00 | 0.02 | 0.00 | 0.02 | 0.01 | 0.00 | 0.01 | 0.00 | 0.02 | 0.03 | 0.02 | 0.03 | 0.02 | 0.02 | 0.02 | 0.01 | 0.03 | 0.03 |
| $CO_2$ | 1.43 | | | 0.17 | | | | | | | | | | | | | | | | | | |
| LOI | 2.95 | 4.98 | 1.47 | 1.44 | 2.98 | 3.46 | 3.52 | 4.71 | 3.87 | 5.28 | 3.30 | 3.33 | 2.97 | 2.67 | 2.96 | 3.10 | 3.56 | 2.85 | 2.95 | 3.01 | 4.15 | 4.74 |
| Total | 99.81 | 100.36 | 100.38 | 99.57 | 100.40 | 99.63 | 100.02 | 100.25 | 99.68 | 100.22 | 100.06 | 100.02 | 100.48 | 100.13 | 99.93 | 99.26 | 100.55 | 100.02 | 100.23 | 99.24 | 99.84 | 99.99 |
| Nb | 4 | 3 | 2 | 2 | 3 | 5 | 5 | 4 | 4 | 3 | 2 | 3 | 4 | 3 | 4 | 3 | 3 | 3 | 3 | 5 | 2 | 4 |
| Zr | 152 | 50 | 102 | 85 | 98 | 131 | 129 | 128 | 128 | 98 | 78 | 73 | 68 | 76 | 73 | 74 | 74 | 70 | 75 | 113 | 65 | 56 |
| Y | 53 | 27 | 37 | 38 | 35 | 41 | 41 | 40 | 40 | 30 | 29 | 27 | 26 | 27 | 26 | 27 | 26 | 26 | 26 | 36 | 25 | 19 |
| Sr | 88 | 61 | 197 | 176 | 166 | 177 | 180 | 180 | 180 | 172 | 248 | 311 | 293 | 245 | 243 | 242 | 312 | 275 | 246 | 202 | 153 | 321 |
| U | 2 | 2 | 2 | 2 | 2 | 2 | 2 | 2 | 2 | 2 | 2 | 2 | 2 | 2 | 2 | 2 | 2 | 2 | 2 | 2 | 2 | 2 |
| Rb | 1 | 1 | 5 | 3 | 3 | 3 | 2 | 3 | 3 | 3 | 8 | 7 | 8 | 8 | 8 | 8 | 7 | 7 | 7 | 2 | 27 | 1 |
| Th | 2 | 5 | 2 | 3 | 2 | 2 | 2 | 2 | 2 | 2 | 2 | 2 | 2 | 2 | 2 | 2 | 2 | 2 | 2 | 2 | 2 | 2 |
| Pb | 6 | 10 | 8 | 7 | 7 | 2 | 2 | 3 | 3 | 3 | 4 | 3 | 2 | 2 | 3 | 3 | 3 | 3 | 4 | 4 | 2 | 19 |
| Ga | 22 | 19 | 17 | 20 | 19 | 19 | 19 | 19 | 19 | 17 | 20 | 19 | 19 | 19 | 19 | 18 | 19 | 18 | 18 | 20 | 12 | 14 |
| Ni | 2 | 68 | 33 | 33 | 22 | 4 | 2 | 4 | 4 | 8 | 29 | 30 | 29 | 31 | 27 | 28 | 30 | 28 | 27 | 8 | 120 | 96 |
| Co | 23 | 48 | 27 | 33 | 35 | 30 | 28 | 28 | 28 | 36 | 24 | 26 | 25 | 26 | 29 | 26 | 27 | 25 | 27 | 37 | 46 | 37 |
| Cr | 26 | 640 | 265 | 91 | 50 | 27 | 16 | 23 | 23 | 37 | 64 | 70 | 74 | 76 | 59 | 67 | 70 | 59 | 73 | 39 | 499 | 349 |
| V | 263 | 315 | 348 | 394 | 420 | 266 | 259 | 246 | 246 | 408 | 352 | 364 | 358 | 350 | 344 | 345 | 352 | 365 | 350 | 493 | 147 | 202 |
| Ba | 24 | 9 | 32 | 40 | 17 | 43 | 51 | 48 | 48 | 24 | 128 | 93 | 125 | 145 | 138 | 129 | 90 | 126 | 139 | 44 | 116 | 30 |
| Hf | 8 | 9 | 8 | 8 | 7 | 5 | 5 | 3 | 3 | 3 | 5 | 1 | 1 | 1 | 5 | 5 | 2 | 1 | 3 | 3 | 4 | 2 |
| Sc | 21 | 62 | 15 | 37 | 30 | 42 | 46 | 40 | 40 | 32 | 47 | 44 | 43 | 49 | 45 | 44 | 39 | 39 | 42 | 62 | 37 | 47 |
| Nb/Y | 0.08 | 0.11 | 0.05 | 0.05 | 0.09 | 0.12 | 0.12 | 0.10 | 0.10 | 0.10 | 0.07 | 0.11 | 0.15 | 0.11 | 0.15 | 0.11 | 0.12 | 0.12 | 0.12 | 0.14 | 0.08 | 0.21 |

Total Fe is expressed as $FeO^*$. Major elements in wt %, trace elements in ppm.

Table 4. Major and trace element analyses of the andesitic volcanic rocks in the Göksun ophiolite, southeastern Turkey

| Sample | K-85 | K-87 | K-88 | K-90 | K-96 | K-99 | K-100 | K-101 | K-102 | K-103 | K-104 | K-105 | K-106 | K-122 | K-144 | K-145 | K-146 | K-219 |
|---|---|---|---|---|---|---|---|---|---|---|---|---|---|---|---|---|---|---|
| $SiO_2$ | 56.36 | 55.74 | 55.82 | 56.77 | 56.06 | 55.85 | 56.18 | 59.56 | 61.67 | 61.27 | 60.66 | 57.90 | 61.05 | 56.36 | 59.13 | 57.24 | 57.98 | 56.47 |
| $TiO_2$ | 1.82 | 1.78 | 1.77 | 1.62 | 1.84 | 2.03 | 2.01 | 1.70 | 1.64 | 1.69 | 1.56 | 1.67 | 1.58 | 1.84 | 1.76 | 1.59 | 1.71 | 0.58 |
| $Al_2O_3$ | 14.71 | 14.57 | 14.58 | 13.89 | 14.80 | 14.26 | 14.27 | 15.28 | 15.51 | 15.81 | 15.63 | 15.30 | 16.01 | 14.91 | 14.40 | 14.31 | 14.13 | 15.28 |
| FeO* | 11.38 | 11.50 | 11.20 | 8.52 | 10.12 | 11.57 | 11.35 | 11.12 | 10.88 | 10.66 | 11.47 | 13.10 | 11.10 | 10.56 | 10.30 | 10.77 | 10.77 | 9.13 |
| MnO | 0.17 | 0.18 | 0.16 | 0.15 | 0.14 | 0.16 | 0.15 | 0.35 | 0.05 | 0.05 | 0.06 | 0.29 | 0.05 | 0.18 | 0.13 | 0.15 | 0.15 | 0.11 |
| MgO | 4.37 | 4.17 | 3.83 | 2.93 | 4.86 | 4.67 | 4.65 | 1.71 | 0.08 | 0.04 | 0.07 | 1.30 | 0.00 | 2.48 | 3.87 | 3.44 | 3.98 | 1.61 |
| CaO | 2.49 | 2.86 | 3.95 | 11.02 | 2.95 | 3.51 | 3.42 | 3.03 | 0.88 | 0.84 | 0.89 | 2.50 | 0.82 | 6.67 | 2.85 | 6.21 | 4.56 | 13.52 |
| $Na_2O$ | 5.23 | 5.36 | 5.21 | 0.26 | 4.15 | 5.65 | 5.61 | 5.92 | 8.80 | 9.23 | 8.79 | 6.19 | 9.40 | 4.13 | 4.50 | 3.76 | 4.17 | 1.61 |
| $K_2O$ | 0.07 | 0.07 | 0.04 | 0.14 | 0.02 | 0.04 | 0.06 | 0.16 | 0.03 | 0.02 | 0.05 | 0.37 | 0.02 | 0.03 | 0.25 | 0.05 | 0.10 | 0.01 |
| $P_2O_5$ | 0.24 | 0.24 | 0.23 | 0.15 | 0.56 | 0.25 | 0.25 | 0.19 | 0.26 | 0.24 | 0.26 | 0.21 | 0.27 | 0.29 | 0.23 | 0.20 | 0.23 | 0.06 |
| $Cr_2O_3$ | 0.00 | 0.00 | 0.00 | 0.00 | 0.00 | 0.00 | 0.00 | 0.05 | 0.08 | 0.05 | 0.08 | 0.04 | 0.09 | 0.03 | 0.01 | 0.02 | 0.05 | 0.08 |
| NiO | 0.00 | 0.00 | 0.00 | 0.00 | 0.00 | 0.00 | 0.00 | 0.02 | 0.03 | 0.02 | 0.04 | 0.02 | 0.04 | 0.01 | 0.00 | 0.00 | 0.02 | 0.03 |
| $CO_2$ | | | | 1.40 | 0.10 | | | | | | | | | | | | | |
| LOI | 3.49 | 3.87 | 3.55 | 3.02 | 4.23 | 2.34 | 2.46 | 1.37 | 0.14 | 0.14 | 0.19 | 1.41 | 0.07 | 2.54 | 2.85 | 2.69 | 2.66 | 1.68 |
| Total | 100.34 | 100.33 | 100.33 | 99.88 | 99.83 | 100.32 | 100.42 | 100.43 | 100.05 | 100.05 | 99.75 | 100.31 | 100.50 | 100.03 | 100.27 | 100.42 | 100.50 | 100.17 |
| Nb | 3 | 4 | 3 | 3 | 4 | 5 | 4 | 5 | 6 | 6 | 5 | 6 | 6 | 5 | 5 | 5 | 6 | 1 |
| Zr | 146 | 148 | 144 | 123 | 146 | 158 | 159 | 111 | 118 | 117 | 119 | 109 | 123 | 130 | 128 | 117 | 128 | 42 |
| Y | 52 | 52 | 51 | 38 | 52 | 52 | 52 | 36 | 27 | 33 | 28 | 38 | 35 | 42 | 43 | 39 | 45 | 19 |
| Sr | 83 | 74 | 109 | 287 | 88 | 75 | 75 | 254 | 97 | 92 | 124 | 200 | 91 | 235 | 161 | 199 | 158 | 417 |
| U | 2 | 2 | 2 | 2 | 2 | 2 | 2 | 2 | 2 | 2 | 2 | 2 | 2 | 2 | 2 | 2 | 2 | 2 |
| Rb | 1 | 1 | 1 | 2 | 1 | 1 | 1 | 3 | 2 | 2 | 2 | 10 | 2 | 3 | 4 | 1 | 2 | 2 |
| Th | 2 | 2 | 2 | 2 | 2 | 2 | 2 | 2 | 2 | 2 | 2 | 2 | 2 | 2 | 2 | 2 | 2 | 2 |
| Pb | 8 | 9 | 6 | 15 | 6 | 2 | 2 | 2 | 2 | 2 | 2 | 6 | 2 | 4 | 2 | 5 | 3 | 13 |
| Ga | 22 | 22 | 22 | 17 | 21 | 19 | 20 | 17 | 9 | 10 | 10 | 14 | 10 | 22 | 16 | 22 | 19 | 17 |
| Ni | 2 | 4 | 5 | 3 | 2 | 46 | 4 | 7 | 8 | 8 | 9 | 22 | 5 | 5 | 5 | 4 | 6 | 37 |
| Co | 33 | 29 | 26 | 23 | 23 | 26 | 18 | 31 | 8 | 7 | 9 | 39 | 5 | 19 | 32 | 32 | 33 | 23 |
| Cr | 98 | 446 | 426 | 24 | 5 | 338 | 264 | 25 | 28 | 27 | 20 | 27 | 25 | 25 | 23 | 41 | 30 | 111 |
| V | 269 | 267 | 252 | 371 | 131 | 297 | 294 | 452 | 275 | 288 | 274 | 274 | 256 | 238 | 371 | 396 | 369 | 278 |
| Ba | 9 | 9 | 9 | 49 | 17 | 10 | 9 | 65 | 64 | 56 | 69 | 78 | 58 | 22 | 88 | 54 | 64 | 12 |
| Hf | 7 | 7 | 6 | 6 | 6 | 8 | 6 | 7 | 5 | 2 | 5 | 5 | 2 | 5 | 6 | 6 | 7 | 5 |
| Sc | 16 | 19 | 16 | 35 | 19 | 11 | 11 | 55 | 41 | 45 | 32 | 48 | 40 | 35 | 52 | 54 | 57 | 25 |
| Nb/Y | 0.06 | 0.08 | 0.06 | 0.08 | 0.08 | 0.10 | 0.08 | 0.14 | 0.22 | 0.18 | 0.18 | 0.16 | 0.17 | 0.12 | 0.12 | 0.13 | 0.13 | 0.05 |

Total Fe is expressed as FeO*. Major elements in wt %, trace elements in ppm.

Table 5. Major and trace element analyses of the dacitic and rhyolitic volcanic rocks in the Göksun ophiolite, southeastern Turkey

| | Dacite | | | | | | | | | | | | | | | | | | | | Rhyolite | |
|---|---|---|---|---|---|---|---|---|---|---|---|---|---|---|---|---|---|---|---|---|---|---|
| Sample | K-107 | K-108 | K-109 | K-110 | K-111 | K-112 | K-113 | K-114 | K-115 | K-116 | K-117 | K-138 | K-139 | K-140 | K-141 | K-142 | K-143 | K-214 | K-215 | K-217 | K-147 | K-148 |
| $SiO_2$ | 65.91 | 64.55 | 64.31 | 65.89 | 64.36 | 63.76 | 64.29 | 65.42 | 64.51 | 62.96 | 64.21 | 64.06 | 63.37 | 63.92 | 63.95 | 63.73 | 64.60 | 63.04 | 69.20 | 65.16 | 77.19 | 75.75 |
| $TiO_2$ | 0.71 | 0.77 | 0.78 | 0.71 | 0.79 | 0.77 | 0.78 | 0.75 | 0.78 | 0.79 | 0.77 | 0.82 | 0.84 | 0.84 | 0.84 | 0.82 | 0.83 | 0.79 | 0.45 | 0.73 | 0.23 | 0.24 |
| $Al_2O_3$ | 14.85 | 16.37 | 16.47 | 14.99 | 16.29 | 15.87 | 16.44 | 15.42 | 15.39 | 16.16 | 15.71 | 15.84 | 15.92 | 15.74 | 15.80 | 15.85 | 15.86 | 15.22 | 13.12 | 14.85 | 11.76 | 11.86 |
| FeO* | 5.48 | 6.04 | 6.02 | 5.60 | 6.04 | 6.04 | 5.98 | 5.77 | 5.96 | 6.18 | 5.93 | 5.73 | 5.83 | 5.93 | 5.90 | 5.80 | 5.79 | 6.90 | 5.58 | 6.15 | 2.10 | 1.90 |
| MnO | 0.13 | 0.15 | 0.14 | 0.14 | 0.13 | 0.14 | 0.13 | 0.14 | 0.19 | 0.21 | 0.11 | 0.12 | 0.12 | 0.12 | 0.12 | 0.12 | 0.12 | 0.16 | 0.11 | 0.15 | 0.09 | 0.08 |
| MgO | 1.20 | 1.37 | 1.31 | 1.24 | 1.29 | 1.35 | 1.37 | 1.35 | 1.69 | 1.79 | 1.49 | 1.59 | 1.73 | 1.68 | 1.71 | 1.64 | 1.67 | 2.10 | 0.89 | 1.92 | 0.77 | 0.89 |
| CaO | 3.72 | 3.47 | 3.39 | 3.76 | 3.72 | 3.67 | 3.68 | 3.78 | 2.73 | 3.07 | 3.69 | 4.78 | 4.49 | 3.94 | 3.82 | 4.12 | 3.98 | 5.60 | 6.67 | 4.75 | 1.40 | 1.63 |
| $Na_2O$ | 5.45 | 4.93 | 4.92 | 5.37 | 5.10 | 4.88 | 5.08 | 5.51 | 5.98 | 6.03 | 5.69 | 5.04 | 4.88 | 5.19 | 4.79 | 5.21 | 5.23 | 4.02 | 2.91 | 4.30 | 5.32 | 5.28 |
| $K_2O$ | 0.06 | 0.36 | 0.38 | 0.06 | 0.28 | 0.30 | 0.33 | 0.08 | 0.12 | 0.10 | 0.06 | 0.17 | 0.51 | 0.33 | 0.63 | 0.29 | 0.35 | 0.11 | 0.05 | 0.12 | 0.18 | 0.20 |
| $P_2O_5$ | 0.23 | 0.24 | 0.25 | 0.23 | 0.25 | 0.24 | 0.24 | 0.24 | 0.25 | 0.26 | 0.25 | 0.24 | 0.23 | 0.25 | 0.24 | 0.24 | 0.25 | 0.12 | 0.08 | 0.11 | 0.04 | 0.04 |
| $Cr_2O_3$ | 0.02 | 0.03 | 0.01 | 0.05 | 0.04 | 0.05 | 0.01 | 0.05 | 0.01 | 0.07 | 0.04 | 0.02 | 0.02 | 0.07 | 0.05 | 0.05 | 0.04 | 0.05 | 0.03 | 0.03 | 0.16 | 0.05 |
| NiO | 0.00 | 0.02 | 0.00 | 0.02 | 0.02 | 0.02 | 0.00 | 0.02 | 0.00 | 0.03 | 0.02 | 0.00 | 0.00 | 0.03 | 0.02 | 0.02 | 0.02 | 0.02 | 0.00 | 0.01 | 0.07 | 0.00 |
| LOI | 1.59 | 2.10 | 2.27 | 1.56 | 1.96 | 1.99 | 2.13 | 1.68 | 1.86 | 1.77 | 1.90 | 1.87 | 2.22 | 1.88 | 1.93 | 1.81 | 1.79 | 2.25 | 1.43 | 2.05 | 0.94 | 1.23 |
| Total | 99.34 | 100.41 | 100.25 | 99.62 | 100.27 | 99.10 | 100.47 | 100.19 | 99.44 | 99.40 | 99.86 | 100.28 | 100.16 | 99.92 | 99.79 | 99.71 | 100.53 | 100.38 | 100.52 | 100.33 | 100.24 | 99.14 |
| Nb | 6 | 6 | 5 | 6 | 5 | 5 | 5 | 6 | 6 | 5 | 6 | 6 | 5 | 5 | 6 | 6 | 6 | 4 | 3 | 3 | 4 | 2 |
| Zr | 143 | 160 | 164 | 143 | 164 | 160 | 160 | 153 | 153 | 164 | 158 | 154 | 160 | 155 | 159 | 153 | 159 | 90 | 58 | 84 | 136 | 139 |
| Y | 42 | 47 | 47 | 41 | 45 | 45 | 46 | 43 | 45 | 47 | 46 | 43 | 45 | 45 | 45 | 45 | 45 | 36 | 26 | 34 | 54 | 52 |
| Sr | 248 | 308 | 307 | 248 | 307 | 314 | 305 | 246 | 195 | 215 | 192 | 175 | 160 | 164 | 157 | 172 | 169 | 254 | 280 | 220 | 133 | 137 |
| U | 2 | 2 | 2 | 2 | 2 | 2 | 2 | 2 | 2 | 2 | 2 | 2 | 2 | 2 | 2 | 2 | 2 | 2 | 2 | 2 | 2 | 2 |
| Rb | 2 | 5 | 6 | 3 | 5 | 5 | 5 | 2 | 3 | 3 | 2 | 4 | 10 | 7 | 13 | 7 | 8 | 3 | 2 | 3 | 6 | 6 |
| Th | 2 | 2 | 2 | 2 | 2 | 2 | 2 | 2 | 2 | 2 | 2 | 2 | 2 | 2 | 2 | 2 | 2 | 2 | 2 | 2 | 3 | 3 |
| Pb | 4 | 2 | 3 | 3 | 2 | 3 | 2 | 3 | 2 | 3 | 2 | 3 | 2 | 3 | 2 | 2 | 3 | 6 | 9 | 7 | 13 | 12 |
| Ga | 16 | 19 | 18 | 16 | 18 | 18 | 18 | 16 | 15 | 16 | 16 | 17 | 17 | 17 | 18 | 18 | 17 | 17 | 14 | 14 | 9 | 9 |
| Ni | 2 | 2 | 2 | 2 | 2 | 3 | 2 | 2 | 2 | 3 | 2 | 4 | 8 | 4 | 3 | 2 | 4 | 16 | 8 | 12 | 2 | 4 |
| Co | 12 | 13 | 13 | 7 | 13 | 14 | 9 | 14 | 13 | 12 | 11 | 9 | 12 | 12 | 10 | 12 | 12 | 15 | 8 | 14 | 5 | 6 |
| Cr | 19 | 12 | 15 | 18 | 14 | 18 | 5 | 12 | 9 | 22 | 9 | 31 | 28 | 11 | 17 | 15 | 25 | 189 | 33 | 36 | 22 | 16 |
| V | 75 | 71 | 70 | 74 | 72 | 72 | 66 | 66 | 60 | 67 | 59 | 86 | 88 | 87 | 86 | 89 | 84 | 111 | 92 | 100 | 14 | 17 |
| Ba | 55 | 95 | 91 | 55 | 92 | 95 | 92 | 61 | 88 | 76 | 71 | 55 | 67 | 63 | 67 | 68 | 52 | 72 | 59 | 84 | 103 | 106 |
| Hf | 6 | 6 | 8 | 6 | 7 | 5 | 10 | 8 | 7 | 9 | 7 | 5 | 5 | 7 | 5 | 7 | 8 | 5 | 7 | 6 | 7 | 7 |
| Sc | 18 | 17 | 16 | 17 | 22 | 20 | 23 | 19 | 27 | 20 | 18 | 21 | 21 | 21 | 22 | 23 | 25 | 26 | 20 | 29 | 9 | 12 |
| Nb/Y | 0.14 | 0.13 | 0.11 | 0.15 | 0.11 | 0.11 | 0.11 | 0.14 | 0.13 | 0.11 | 0.13 | 0.14 | 0.11 | 0.11 | 0.13 | 0.13 | 0.13 | 0.11 | 0.12 | 0.09 | 0.07 | 0.04 |

Total Fe is expressed as FeO*. Major elements in wt %, trace elements in ppm.

Table 6. Major and trace element analyses of the sheeted dyke rocks in the Göksun ophiolite, southeastern Turkey

| Samples | K-6 | K-7 | K-8 | K-9 | K-11 | K-16 | K-17 | K-18 | K-19 | K-20 | K-21 | K-26 | K-27 | K-31 | K-32 | K-60 | K-63 | K 154 | K 155 | K 156 | K 157 | K 158 |
|---|---|---|---|---|---|---|---|---|---|---|---|---|---|---|---|---|---|---|---|---|---|---|
| $SiO_2$ | 53.38 | 53.80 | 50.94 | 55.35 | 52.33 | 49.17 | 51.42 | 48.57 | 54.57 | 51.56 | 53.44 | 51.78 | 57.66 | 50.61 | 50.38 | 62.10 | 49.59 | 52.95 | 51.11 | 52.89 | 48.94 | 50.52 |
| $TiO_2$ | 1.95 | 1.43 | 0.84 | 1.80 | 1.66 | 1.69 | 1.69 | 1.00 | 1.89 | 1.72 | 0.92 | 1.33 | 1.69 | 0.93 | 1.00 | 0.67 | 0.52 | 2.18 | 1.32 | 1.72 | 1.32 | 1.80 |
| $Al_2O_3$ | 13.80 | 15.28 | 16.97 | 13.77 | 15.34 | 15.15 | 15.34 | 16.47 | 14.09 | 14.93 | 15.12 | 15.23 | 12.70 | 16.16 | 16.55 | 17.14 | 16.61 | 14.02 | 15.57 | 14.67 | 16.31 | 14.60 |
| FeO* | 11.75 | 9.62 | 7.33 | 10.69 | 11.67 | 13.36 | 12.16 | 8.44 | 10.64 | 11.50 | 8.93 | 10.71 | 10.64 | 8.27 | 8.32 | 5.72 | 7.98 | 12.71 | 12.07 | 13.61 | 12.46 | 13.50 |
| MnO | 0.18 | 0.11 | 0.11 | 0.16 | 0.20 | 0.23 | 0.21 | 0.17 | 0.16 | 0.21 | 0.17 | 0.19 | 0.12 | 0.16 | 0.13 | 0.17 | 0.15 | 0.12 | 0.17 | 0.13 | 0.14 | 0.15 |
| MgO | 5.41 | 3.08 | 7.92 | 3.32 | 5.09 | 5.52 | 5.10 | 6.10 | 3.28 | 5.01 | 6.90 | 5.61 | 4.12 | 7.93 | 7.45 | 2.21 | 7.77 | 4.77 | 6.44 | 4.50 | 7.25 | 4.15 |
| CaO | 8.52 | 14.31 | 11.38 | 10.50 | 5.11 | 5.89 | 5.30 | 12.74 | 10.80 | 7.52 | 7.04 | 7.13 | 8.83 | 11.50 | 11.27 | 6.83 | 12.24 | 6.41 | 5.36 | 5.34 | 4.75 | 11.12 |
| $Na_2O$ | 0.03 | 0.24 | 2.64 | 0.01 | 4.94 | 3.77 | 4.67 | 2.44 | 0.01 | 4.16 | 4.75 | 3.84 | 0.36 | 2.52 | 2.82 | 4.06 | 1.66 | 5.76 | 4.25 | 4.83 | 5.21 | 0.74 |
| K2O | 0.01 | 0.00 | 0.03 | 0.01 | 0.01 | 0.01 | 0.02 | 0.01 | 0.01 | 0.02 | 0.25 | 0.44 | 0.01 | 0.16 | 0.14 | 0.06 | 0.04 | 0.03 | 0.31 | 0.09 | 0.04 | 0.01 |
| $P_2O_5$ | 0.18 | 0.18 | 0.08 | 0.21 | 0.15 | 0.14 | 0.16 | 0.09 | 0.16 | 0.14 | 0.09 | 0.11 | 0.15 | 0.09 | 0.08 | 0.12 | 0.04 | 0.17 | 0.13 | 0.16 | 0.12 | 0.16 |
| $Cr_2O_3$ | 0.01 | 0.01 | 0.03 | 0.00 | 0.00 | 0.00 | 0.00 | 0.03 | 0.00 | 0.00 | 0.03 | 0.01 | 0.00 | 0.04 | 0.04 | 0.00 | 0.04 | 0.06 | 0.01 | 0.04 | 0.02 | 0.02 |
| NiO | 0.00 | 0.00 | 0.01 | 0.00 | 0.00 | 0.00 | 0.00 | 0.01 | 0.00 | 0.00 | 0.01 | 0.00 | 0.00 | 0.01 | 0.01 | 0.00 | 0.01 | 0.02 | 0.00 | 0.01 | 0.00 | 0.00 |
| $CO_2$ | 0.10 | 0.15 | 0.20 | 0.13 | 0.00 | 0.60 | 0.30 | 0.50 | 0.15 | 0.10 | 0.16 | 0.30 | 0.14 | 0.13 | 0.10 | 0.10 | 0.10 | | | | | |
| LOI | 4.62 | 1.26 | 1.35 | 3.49 | 3.41 | 4.13 | 3.42 | 3.23 | 3.82 | 3.00 | 2.48 | 2.66 | 3.40 | 1.55 | 1.49 | 0.75 | 3.23 | 1.26 | 2.90 | 2.51 | 3.76 | 3.19 |
| Total | 99.94 | 99.47 | 99.84 | 99.43 | 99.90 | 99.66 | 99.80 | 99.80 | 99.58 | 99.86 | 100.31 | 99.35 | 99.80 | 100.06 | 99.78 | 99.92 | 99.98 | 100.45 | 99.63 | 100.49 | 100.32 | 99.97 |
| Nb | 4 | 2 | 1 | 4 | 3 | 4 | 4 | 1 | 4 | 3 | 3 | 1 | 4 | 1 | 1 | 1 | 1 | 5 | 4 | 5 | 4 | 4 |
| Zr | 126 | 136 | 53 | 127 | 96 | 97 | 104 | 62 | 120 | 89 | 59 | 82 | 107 | 61 | 57 | 67 | 28 | 110 | 71 | 98 | 71 | 107 |
| Y | 43 | 33 | 22 | 43 | 40 | 37 | 38 | 23 | 38 | 34 | 28 | 30 | 41 | 21 | 22 | 34 | 17 | 35 | 27 | 33 | 29 | 31 |
| Sr | 254 | 258 | 137 | 281 | 82 | 92 | 85 | 195 | 293 | 102 | 180 | 153 | 252 | 171 | 140 | 224 | 119 | 67 | 136 | 126 | 67 | 274 |
| U | 2 | 2 | 2 | 2 | 2 | 3 | 2 | 2 | 2 | 2 | 2 | 2 | 2 | 2 | 2 | 2 | 2 | 2 | 2 | 2 | 2 | 2 |
| Rb | 1 | 1 | 3 | 1 | 1 | 1 | 1 | 1 | 1 | 1 | 3 | 10 | 1 | 6 | 5 | 1 | 2 | 3 | 7 | 4 | 2 | 3 |
| Th | 2 | 2 | 2 | 2 | 2 | 2 | 2 | 2 | 2 | 2 | 2 | 2 | 2 | 2 | 2 | 2 | 2 | 2 | 2 | 2 | 2 | 2 |
| Pb | 17 | 17 | 12 | 18 | 6 | 10 | 7 | 13 | 16 | 11 | 9 | 11 | 16 | 11 | 10 | 7 | 13 | 2 | 6 | 7 | 4 | 9 |
| Ga | 17 | 18 | 16 | 17 | 19 | 20 | 20 | 18 | 18 | 19 | 16 | 20 | 16 | 17 | 17 | 18 | 16 | 15 | 17 | 19 | 17 | 18 |
| Ni | 16 | 31 | 77 | 10 | 4 | 9 | 3 | 62 | 10 | 12 | 67 | 19 | 9 | 87 | 72 | 2 | 67 | 12 | 24 | 9 | 30 | 9 |
| Co | 44 | 33 | 42 | 35 | 27 | 55 | 43 | 42 | 37 | 38 | 41 | 40 | 44 | 43 | 41 | 12 | 42 | 30 | 42 | 39 | 40 | 42 |
| Cr | 32 | 83 | 200 | 14 | 14 | 23 | 49 | 178 | 33 | 22 | 227 | 280 | 72 | 283 | 282 | 12 | 213 | 34 | 65 | 44 | 198 | 35 |
| V | 372 | 282 | 217 | 295 | 430 | 428 | 438 | 260 | 401 | 425 | 300 | 383 | 355 | 248 | 267 | 49 | 274 | 511 | 397 | 438 | 378 | 422 |
| Ba | 38 | 46 | 15 | 32 | 26 | 25 | 37 | 12 | 33 | 39 | 35 | 97 | 35 | 42 | 26 | 43 | 44 | 9 | 72 | 23 | 27 | 9 |
| Hf | 6 | 5 | 7 | 5 | 6 | 7 | 5 | 7 | 6 | 7 | 8 | 6 | 6 | 5 | 6 | 6 | 6 | 6 | 6 | 4 | 3 | 8 |
| Sc | 44 | 33 | 41 | 33 | 31 | 33 | 30 | 37 | 40 | 27 | 36 | 30 | 38 | 41 | 38 | 23 | 54 | 49 | 64 | 66 | 85 | 54 |
| Nb/Y | 0.09 | 0.06 | 0.05 | 0.09 | 0.08 | 0.11 | 0.11 | 0.04 | 0.11 | 0.09 | 0.11 | 0.03 | 0.10 | 0.05 | 0.05 | 0.03 | 0.06 | 0.14 | 0.15 | 0.15 | 0.14 | 0.13 |

Total Fe is expressed as FeO*. Major elements in wt %, trace elements in ppm.

Table 7. Major and trace element analyses of the isotropic gabbroic rocks in the Göksun ophiolite, southeastern Turkey

| Samples | K-10 | K-12 | K-13 | K-14 | K-15 | K-22 | K-23 | K-24 | K-25 | K-159 | K-160 | K-161 | K-162 |
|---|---|---|---|---|---|---|---|---|---|---|---|---|---|
| $SiO_2$ | 60.19 | 61.77 | 61.30 | 60.37 | 63.07 | 50.59 | 67.73 | 61.61 | 64.07 | 63.61 | 63.82 | 63.62 | 64.36 |
| $TiO_2$ | 1.43 | 1.30 | 1.29 | 1.41 | 1.22 | 0.94 | 0.96 | 1.34 | 0.96 | 1.17 | 1.23 | 1.14 | 0.93 |
| $Al_2O_3$ | 15.81 | 14.26 | 15.05 | 15.02 | 14.09 | 15.86 | 14.59 | 14.94 | 14.77 | 14.73 | 14.57 | 14.33 | 14.38 |
| FeO* | 6.77 | 7.97 | 8.21 | 8.49 | 6.54 | 8.50 | 2.91 | 6.64 | 5.36 | 5.31 | 6.10 | 5.98 | 5.16 |
| MnO | 0.12 | 0.16 | 0.14 | 0.15 | 0.18 | 0.14 | 0.05 | 0.07 | 0.05 | 0.06 | 0.06 | 0.06 | 0.05 |
| MgO | 2.74 | 2.05 | 1.88 | 2.00 | 2.12 | 6.94 | 1.54 | 1.95 | 1.76 | 1.73 | 1.62 | 1.75 | 1.40 |
| CaO | 5.06 | 4.28 | 3.83 | 4.09 | 5.15 | 9.61 | 4.57 | 5.77 | 5.39 | 5.81 | 5.64 | 5.42 | 5.98 |
| $Na_2O$ | 5.14 | 6.11 | 6.03 | 5.96 | 5.91 | 3.93 | 6.67 | 5.99 | 6.08 | 6.02 | 6.42 | 5.66 | 5.78 |
| $K_2O$ | 0.01 | 0.05 | 0.16 | 0.17 | 0.16 | 0.00 | 0.17 | 0.02 | 0.20 | 0.27 | 0.12 | 0.40 | 0.29 |
| $P_2O_5$ | 0.30 | 0.42 | 0.36 | 0.36 | 0.39 | 0.10 | 0.24 | 0.23 | 0.24 | 0.22 | 0.22 | 0.21 | 0.24 |
| $Cr_2O_3$ | 0.00 | 0.00 | 0.00 | 0.00 | 0.00 | 0.03 | 0.00 | 0.00 | 0.00 | 0.07 | 0.11 | 0.10 | 0.11 |
| NiO | 0.00 | 0.00 | 0.00 | 0.00 | 0.00 | 0.01 | 0.00 | 0.00 | 0.00 | 0.03 | 0.05 | 0.05 | 0.05 |
| $CO_2$ | 0.00 | 0.11 | 0.25 | 0.24 | 0.15 | 0.10 | 0.13 | 0.17 | 0.17 | | | | |
| LOI | 2.40 | 1.36 | 1.37 | 1.41 | 1.10 | 3.40 | 0.55 | 0.98 | 0.64 | 0.50 | 0.41 | 1.21 | 0.47 |
| Total | 99.98 | 99.83 | 99.86 | 99.65 | 100.07 | 100.15 | 100.12 | 99.71 | 99.69 | 99.53 | 100.38 | 99.92 | 99.20 |
| Nb | 4 | 4 | 3 | 3 | 4 | 1 | 4 | 2 | 3 | 4 | 5 | 5 | 5 |
| Zr | 147 | 168 | 185 | 170 | 177 | 61 | 187 | 147 | 197 | 174 | 166 | 163 | 184 |
| Y | 65 | 78 | 69 | 67 | 73 | 27 | 87 | 46 | 71 | 60 | 64 | 55 | 67 |
| Sr | 148 | 79 | 141 | 146 | 122 | 96 | 136 | 125 | 173 | 148 | 130 | 142 | 160 |
| U | 2 | 2 | 2 | 3 | 2 | 2 | 2 | 2 | 2 | 2 | 2 | 2 | 2 |
| Rb | 1 | 1 | 1 | 1 | 1 | 1 | 1 | 1 | 2 | 6 | 3 | 9 | 6 |
| Th | 2 | 3 | 2 | 2 | 2 | 2 | 2 | 2 | 2 | 2 | 2 | 2 | 2 |
| Pb | 4 | 4 | 4 | 3 | 4 | 8 | 2 | 2 | 4 | 2 | 2 | 2 | 3 |
| Ga | 21 | 21 | 21 | 22 | 18 | 18 | 19 | 20 | 21 | 17 | 18 | 18 | 19 |
| Ni | 2 | 2 | 2 | 2 | 2 | 69 | 2 | 2 | 2 | 4 | 2 | 3 | 4 |
| Co | 24 | 18 | 15 | 18 | 18 | 41 | 9 | 8 | 11 | 12 | 10 | 9 | 8 |
| Cr | 18 | 17 | 17 | 8 | 18 | 246 | 18 | 8 | 10 | 28 | 29 | 26 | 21 |
| V | 65 | 55 | 43 | 52 | 61 | 276 | 23 | 45 | 50 | 98 | 77 | 54 | 45 |
| Ba | 9 | 9 | 33 | 33 | 22 | 17 | 46 | 9 | 39 | 75 | 46 | 104 | 76 |
| Hf | 6 | 5 | 7 | 5 | 6 | 7 | 5 | 6 | 6 | 7 | 7 | 5 | 7 |
| Sc | 13 | 12 | 5 | 6 | 8 | 37 | 3 | 10 | 5 | 17 | 18 | 24 | 18 |
| Nb/Y | 0.06 | 0.05 | 0.04 | 0.04 | 0.05 | 0.04 | 0.05 | 0.04 | 0.04 | 0.07 | 0.08 | 0.09 | 0.07 |

Total Fe is expressed as FeO*. Major elements in wt %, trace elements in ppm.

LILE) mobility during alteration processes. Figure 7 presents the comparisons of K and Ba against Zr in order to test element mobility. K and Ba show non-systematic scattered distribution when plotted against Zr, reflecting their mobility, and they are therefore not reliable as indicators of petrogenetic relationships.

Immobile element variations are shown in Figure 8. The Zr v. Y diagrams (Fig. 8a, c) display characteristic linear positive relationships, suggesting a co-magmatic origin for these rocks. Ti v. Zr diagrams for the volcanic rocks, sheeted dykes and isotropic gabbros are presented in Figure 8b and d. The main characteristics of these diagrams are (a) the positive correlations of Ti and Zr for basic to intermediate rock units, consistent with a crystallizing assemblage of olivine, clinopyroxene and plagioclase (Pearce & Norry, 1979; Pearce, 1982); (b) a sudden fall in Ti/Zr ratios of volcanic and plutonic rocks during fractionation. Magnetite/titanomagnetite crystallization is the most important cause of decreasing Ti concentration relative to Zr during fractionation (Winchester & Floyd, 1977; Pearce, 1982). All the interelement relations based on immobile elements suggest that the volcanic and plutonic units of the Göksun ophiolite show similar geochemical features, consistent with co-magmatic relationships during the formation of the oceanic crust in southern Neotethyan ocean basin.

The chondrite-normalized REE patterns of the crustal rocks of the Göksun ophiolite are shown in Figure 9a, b. Total REE contents of the volcanic rocks range from 4 to 50 times chondritic. The volcanic rocks present mainly flat-lying REE patterns ($[La/Yb]_N = 0.8–1.8$) with the exception of two samples. One basaltic sample shows an LREE depleted pattern ($[La/Yb]_N = 0.5$), whereas a dacite displays a LREE enriched pattern ($[La/Yb]_N = 2.2$) (Fig. 9a). The intermediate and acidic lavas (andesite to rhyolite) display a pronounced negative Eu anomaly (Fig. 9a), which is a consequence of the removal of feldspar by fractional crystallization or the partial melting of a rock in which feldspar is retained in the source (Rollinson, 1993). The sheeted dykes and isotropic gabbros have similar flat REE patterns ($[La/Yb]_N = 0.8–1.0$ and 1.2–1.4, respectively) (Fig. 9b), confirming a possible co-magmatic relationship of the crustal rocks. Flat REE patterns are typically found in island arc tholeiitic series, namely in Papua New Guinea, Solomon Islands, Macquarie Island (Jakes & Gill, 1970), and suprasubduction zone-type ophiolites of the eastern Mediterranean (Alabaster, Pearce & Malpas, 1982; Parlak, 1996; Yalınız, Floyd & Göncüoğlu, 1996; Parlak, Höck & Delaloye, 2000; Al-Riyami *et al*. 2002).

The N-MORB normalized spider diagrams of the rock units from the volcanic rocks, sheeted dykes

https://doi.org/10.1017/S0016756804009458 Published online by Cambridge University Press

Table 8. Trace element and REE compositions of the subset of the Göksun ophiolite samples analysed by ICP-MS

| | Basalt | | | Bas-andesite | | Andesite | | | Dacite | Rhyolite | Sheeted Dykes | | | | Isotropic gabbro | | |
|---|---|---|---|---|---|---|---|---|---|---|---|---|---|---|---|---|---|
| Sample | K-93 | K-81 | K-124 | K-86 | K-132 | K-99 | K-104 | K-145 | K-112 | K-148 | K-8 | K-20 | K-31 | K-156 | K-14 | K-23 | K-161 |
| Th | 0.32 | 0.35 | 0.49 | 0.62 | 0.68 | 0.5 | 0.51 | 0.37 | 1.43 | 0.91 | 0.34 | 0.3 | 0.37 | 0.44 | 0.83 | 0.78 | 0.80 |
| U | 0.07 | 0.05 | 0.61 | 0.16 | 0.59 | 0.13 | 0.62 | 0.82 | 0.85 | 0.75 | 0.07 | 0.07 | 0.05 | 0.45 | 0.19 | 0.2 | 0.58 |
| Nb | 2 | 1.3 | 2.1 | 2.7 | 2.7 | 2.7 | 2.1 | 1.7 | 3.4 | 1.6 | 1.9 | 2.1 | 1.7 | 1.7 | 3.6 | 3.3 | 2.6 |
| Hf | 2.3 | 1.1 | 3.0 | 4.4 | 1.8 | 4.3 | 3.0 | 3.0 | 3.5 | 4.8 | 1.5 | 2.4 | 1.7 | 2.5 | 5.3 | 5.7 | 5.2 |
| Ta | < | < | 0.14 | 0.1 | 0.19 | 0.1 | 0.13 | 0.10 | 0.26 | 0.11 | < | < | < | 0.11 | 0.1 | 0.1 | 0.17 |
| Zr | 87 | 32 | 99 | 150 | 64 | 144 | 95 | 96 | 120 | 157 | 53 | 83 | 65 | 84 | 189 | 192 | 171 |
| Y | 32.9 | 14.1 | 42.2 | 46.8 | 23.9 | 46.1 | 29.9 | 40.4 | 39.3 | 43.6 | 19.8 | 29.6 | 20.5 | 37.1 | 60.4 | 71.3 | 58.4 |
| La | 3.81 | 1.09 | 6.37 | 6.61 | 6.49 | 5.98 | 5.49 | 5.23 | 13.3 | 7.91 | 2.64 | 3.41 | 2.44 | 5.40 | 9.8 | 11.9 | 11.3 |
| Ce | 10.4 | 3.1 | 18.0 | 18.8 | 14.9 | 17.3 | 13.7 | 16.1 | 31.4 | 20.7 | 6.7 | 9.9 | 7 | 14.3 | 27.3 | 35.7 | 32.5 |
| Pr | 1.67 | 0.53 | 2.66 | 2.85 | 1.83 | 2.7 | 1.98 | 2.39 | 3.79 | 2.68 | 1.05 | 1.55 | 1.08 | 2.15 | 4.13 | 5.31 | 4.23 |
| Nd | 9.47 | 3.16 | 15.3 | 16.1 | 9.50 | 15.2 | 11.5 | 13.2 | 18.3 | 14.0 | 6.06 | 9.13 | 6.52 | 12.1 | 22.9 | 28 | 21.3 |
| Sm | 3.14 | 1.27 | 4.65 | 5.26 | 2.74 | 5.15 | 3.41 | 4.22 | 4.95 | 4.14 | 2.01 | 3.1 | 2.11 | 4.06 | 6.96 | 8.21 | 6.17 |
| Eu | 1.19 | 0.535 | 1.92 | 1.8 | 1.04 | 1.6 | 0.869 | 1.88 | 1.64 | 0.826 | 0.834 | 1.35 | 0.898 | 1.51 | 2.2 | 2.54 | 2.40 |
| Gd | 4.02 | 1.75 | 6.51 | 6.74 | 3.58 | 6.64 | 4.57 | 5.96 | 5.88 | 5.11 | 2.72 | 4.03 | 2.78 | 5.15 | 8.66 | 10 | 8.14 |
| Tb | 0.82 | 0.34 | 1.17 | 1.21 | 0.64 | 1.17 | 0.81 | 1.06 | 1.03 | 1.08 | 0.52 | 0.75 | 0.5 | 0.94 | 1.54 | 1.88 | 1.49 |
| Dy | 5 | 2.22 | 7.19 | 7.84 | 4.04 | 7.59 | 5.35 | 6.65 | 6.63 | 7.07 | 3.11 | 4.86 | 3.29 | 6.41 | 9.76 | 11.6 | 9.42 |
| Ho | 1.1 | 0.49 | 1.48 | 1.64 | 0.84 | 1.64 | 1.12 | 1.43 | 1.41 | 1.53 | 0.7 | 1.04 | 0.7 | 1.35 | 2.06 | 2.49 | 2.03 |
| Er | 3.35 | 1.52 | 4.59 | 4.97 | 2.64 | 4.9 | 3.77 | 4.33 | 4.38 | 5.04 | 2.09 | 3.13 | 2.11 | 3.97 | 6.27 | 7.56 | 6.47 |
| Tm | 0.502 | 0.221 | 0.699 | 0.766 | 0.407 | 0.743 | 0.600 | 0.632 | 0.652 | 0.846 | 0.307 | 0.479 | 0.31 | 0.600 | 0.922 | 1.18 | 0.924 |
| Yb | 3.13 | 1.5 | 4.12 | 4.62 | 2.55 | 4.5 | 3.73 | 3.92 | 4.32 | 5.47 | 1.84 | 2.89 | 1.89 | 3.92 | 5.68 | 7.19 | 6.00 |
| Lu | 0.49 | 0.243 | 0.609 | 0.766 | 0.374 | 0.739 | 0.549 | 0.580 | 0.645 | 0.844 | 0.305 | 0.482 | 0.309 | 0.601 | 0.911 | 1.14 | 0.909 |
| Th/Yb | 0.10 | 0.23 | 0.12 | 0.13 | 0.27 | 0.11 | 0.14 | 0.09 | 0.33 | 0.17 | 0.18 | 0.10 | 0.20 | 0.11 | 0.15 | 0.11 | 0.13 |
| Ta/Yb | – | – | 0.03 | 0.02 | 0.08 | 0.02 | 0.03 | 0.03 | 0.06 | 0.02 | – | – | – | 0.03 | 0.02 | 0.01 | 0.03 |
| La/Ta | – | – | 46.86 | 66.10 | 33.79 | 59.80 | 42.36 | 52.64 | 50.73 | 74.68 | – | – | – | 48.11 | 98.00 | 119.00 | 65.53 |
| Nb/Th | 6.25 | 3.71 | 4.25 | 4.35 | 3.92 | 5.40 | 4.04 | 4.58 | 2.41 | 1.78 | 5.59 | 7.00 | 4.59 | 3.88 | 4.34 | 4.23 | 3.29 |
| Nb/Y | 0.06 | 0.09 | 0.05 | 0.06 | 0.11 | 0.06 | 0.07 | 0.04 | 0.09 | 0.04 | 0.10 | 0.07 | 0.08 | 0.05 | 0.06 | 0.05 | 0.05 |
| Hf/Th | 7.19 | 3.14 | 6.21 | 7.10 | 2.71 | 8.60 | 5.80 | 8.09 | 2.46 | 5.22 | 4.41 | 8.00 | 4.59 | 5.75 | 6.39 | 7.31 | 6.51 |
| Zr/Y | 2.64 | 2.27 | 2.35 | 3.21 | 2.67 | 3.12 | 3.19 | 2.38 | 3.06 | 3.60 | 2.68 | 2.80 | 3.17 | 2.27 | 3.13 | 2.69 | 2.93 |

< = below detection limit; – = not available.

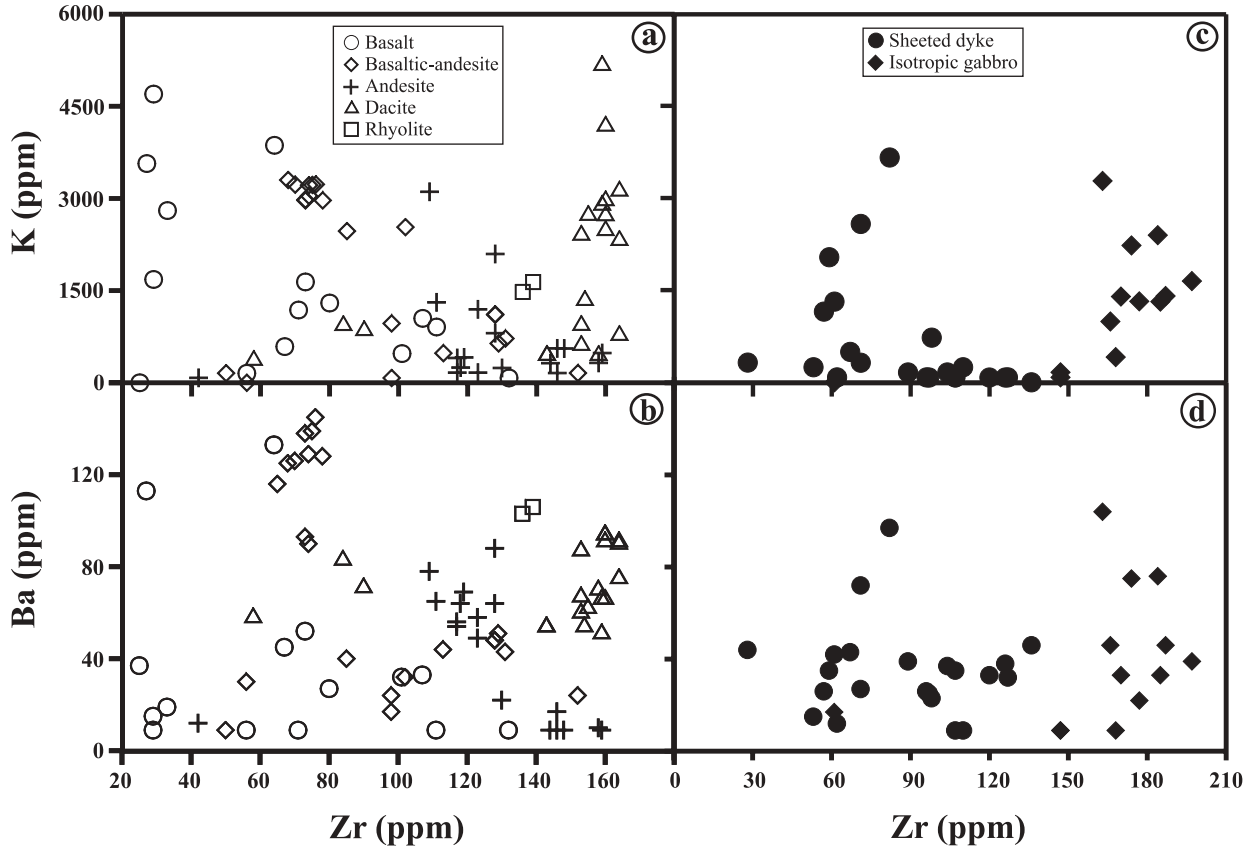


Figure 7. Identification of chemical alteration of the volcanic rocks (a), sheeted dyke and isotropic gabbroic rocks (b) in the Göksun ophiolite.

and isotropic gabbros are presented in Figure 10a–d. The main features of these diagrams are that (a) they have nearly flat-lying patterns (except LIL element enrichment such as Rb, Ba, Th), (b) large negative Nb (Ta) anomalies through all rock series and (c) negative Ti and P anomalies in intermediate to silicic rocks. The LIL element enrichment is thought to be related to the transfer of elements from the subducted plate to the overlying mantle wedge. The elevated concentrations of LILE relative to HFSE in subduction zone magmas originate from fluids and/or siliceous melts derived from the subducting oceanic slab. These slab-derived fluids carry high concentrations of LILE while the HFSE, most notably Ta and Nb, are retained in the slab (Pearce, 1982; Arculus & Powell, 1986; Yogodzinski *et al*. 1993; Wallin & Metcalf, 1998). Therefore the negative Nb (Ta) anomaly is clearly intrinsic to the Göksun ophiolite parental magma and is not an artefact of crystallization processes. Within the LIL element group, Th is a relatively stable and reliable indicator, whose enrichment relative to other incompatible elements is taken to represent the subduction zone component (Wood, Joron & Treuil, 1979; Pearce, 1983). The negative Nb (Ta) and positive Th anomalies obtained from the Göksun ophiolite rocks clearly indicate a suprasubduction zone tectonic environment. The negative Ti and P anomalies are restricted to the intermediate and silicic rocks of the Göksun ophiolite and are not observed in less differentiated rocks. It is clear that the Ti and P anomalies are related to the onset of Fe–Ti oxide and apatite crystallization (Elthon, 1991).

To show the arc signature of the crustal rocks from the Göksun ophiolite, Nb/Th is plotted against Y in Figure 11a (after Jenner *et al*. 1991). The volcanic rocks, sheeted dykes and the isotropic gabbros plot well within the arc field. On a Th/Yb v. Ta/Yb ratio–ratio plot, designed to discriminate between depleted mantle (MORB) and enriched mantle (intraplate) sources for subduction related magmatic rocks (Pearce, 1982), data from the mafic and felsic crustal rocks of the Göksun ophiolite are consistent with derivation from a MORB-type depleted mantle source enriched by subduction zone fluids (Fig. 11b). This evidence again supports the co-magmatic origin of the crustal rocks in the Göksun ophiolite. A Hf–Th–Ta (Nb) triangular diagram for basic to silicic volcanic rocks erupted in different tectonic settings was proposed by Wood, Joron & Treuil (1979). The rocks of the Göksun ophiolite plot close to the island arc basalts and differentiates field (Fig. 12a, b), suggesting a suprasubduction zone tectonic setting for its origin.

https://doi.org/10.1017/S0016756804009458 Published online by Cambridge University Press

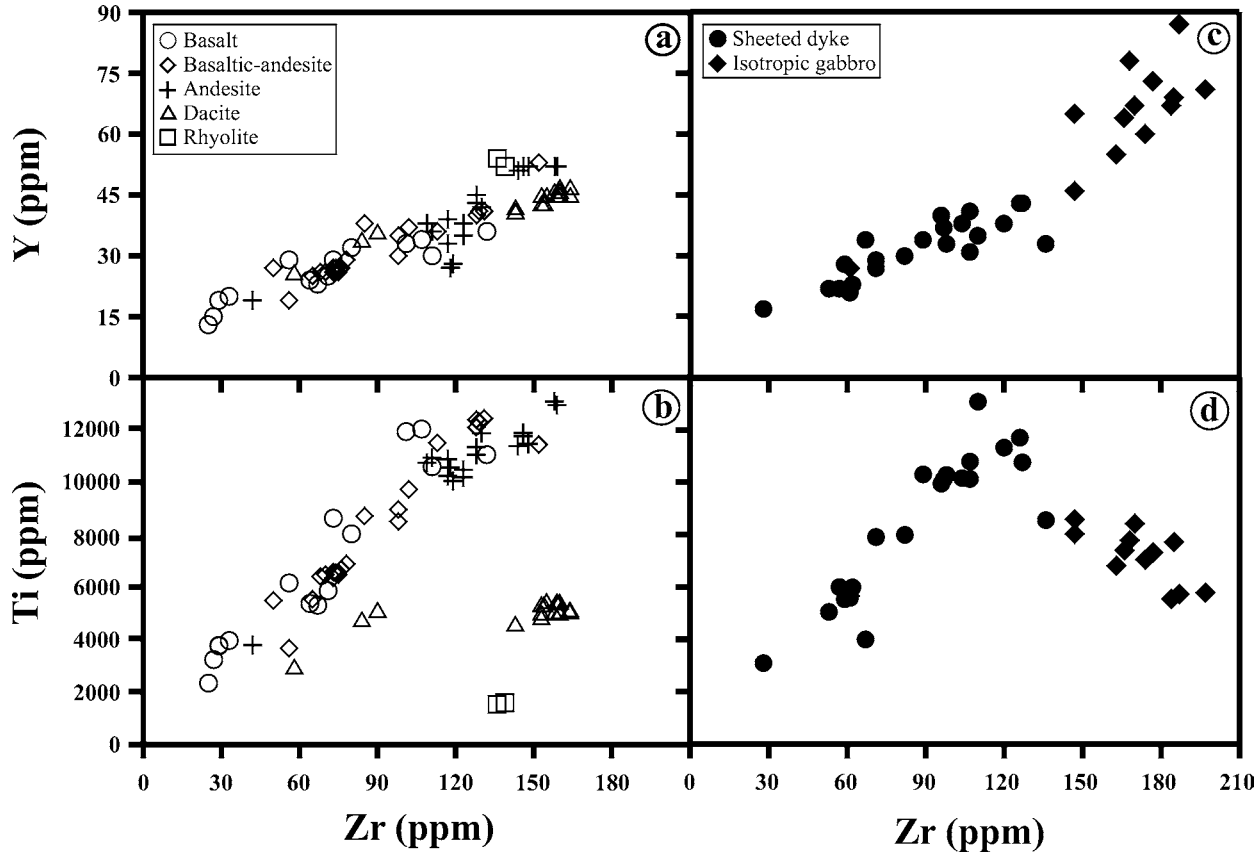


Figure 8. Variation of immobile (Y and Ti) trace elements relative to Zr for the volcanic rocks (a, b), sheeted dykes and isotropic gabbros (c, d) of the Göksun ophiolite.

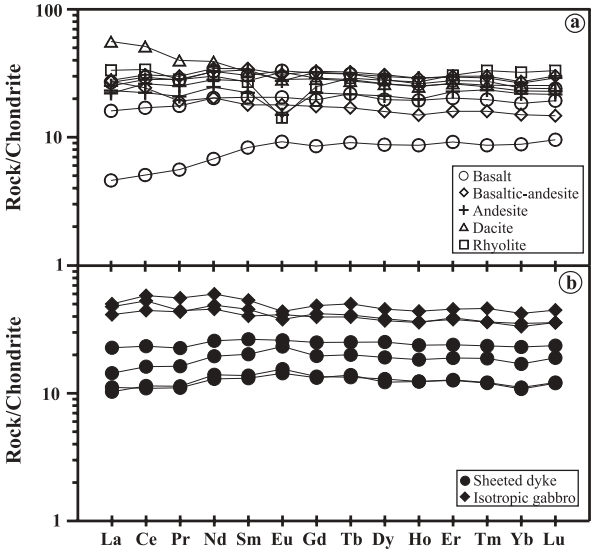


Figure 9. Chondrite normalized REE patterns of the volcanic rocks (a), sheeted dykes and isotropic gabbros (b) of the Göksun ophiolite (normalizing values are from Sun & McDonough, 1989).

## 6. Discussion

The eastern Mediterranean ophiolites in southeastern Turkey form discontinuous linear belts of oceanic fragments immediately north of the Bitlis–Zagros suture, which marks a continental collision zone between the Arabian platform to the south and the Taurides to the north. In southeast Anatolia there are number of tectonomagmatic entities that are important in understanding the geological evolution of the region during the Late Cretaceous–Early Tertiary period. These are (a) the active margin units, (b) the ophiolitic bodies, (c) the high-grade metamorphic sole rocks and (d) the volcanic–sedimentary units. The active margin, called the Baskil arc (Aktaş & Robertson, 1984; Yazgan & Chessex, 1991) or Elazığ magmatics (Beyarslan & Bingöl, 2000), predominantly comprises plutonic rocks (gabbros and diorites to granodiorites and tonalities) and calc-alkaline volcanic rocks of Coniacian to early Campanian age (Yazgan & Chessex, 1991; Parlak *et al*. 2001). The Baskil arc magmatics intrude the Malatya–Keban platform, ophiolites and related metamorphic rock units in the region. Geological and petrological data suggest that the Baskil magmatic arc was a typical Andean-type active continental margin that occurred as a result of N-dipping subduction beneath the Malatya–Keban platform (Yazgan & Chessex, 1991). The Late Cretaceous ophiolitic bodies of southeast Anatolia are represented by Göksun in the north of Kahramanmaraş, and İspendere–Kömürhan–Guleman near Hazar Lake, a pull-apart basin along the East Anatolian Fault Zone (Dunne & Hempton, 1984) in Elazığ. The Kömürhan

https://doi.org/10.1017/S0016756804009458 Published online by Cambridge University Press

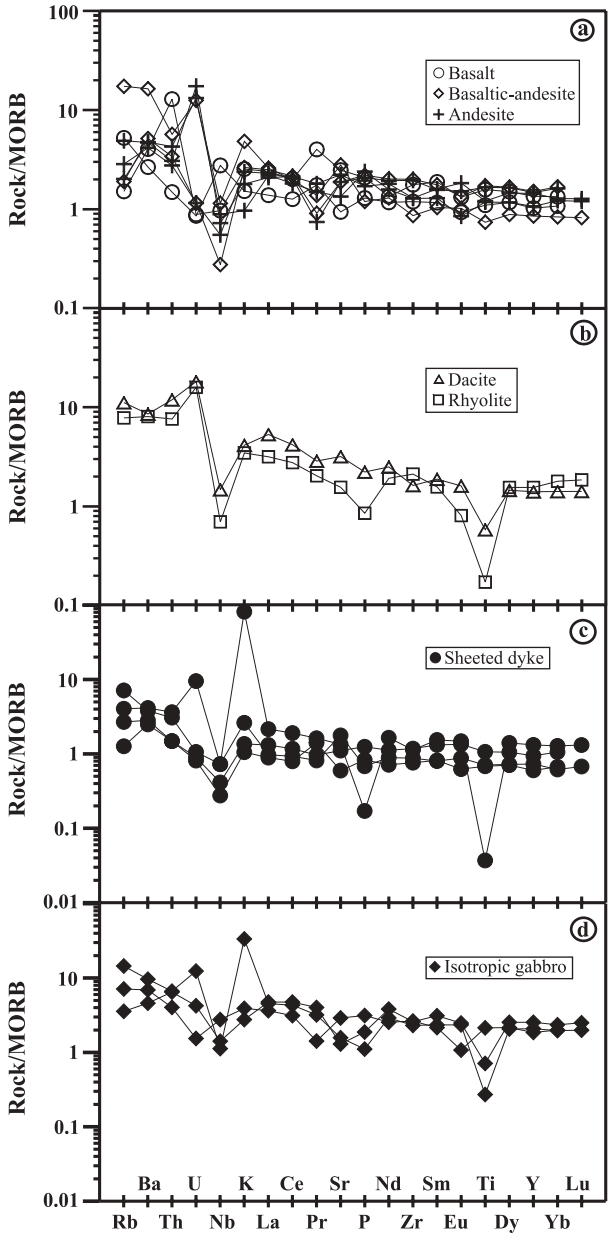


Figure 10. N-MORB normalized spider diagram for the volcanic rocks (a, b), sheeted dykes (c) and isotropic gabbros (d) of the Göksun ophiolite (normalizing values are from Sun & McDonough, 1989).

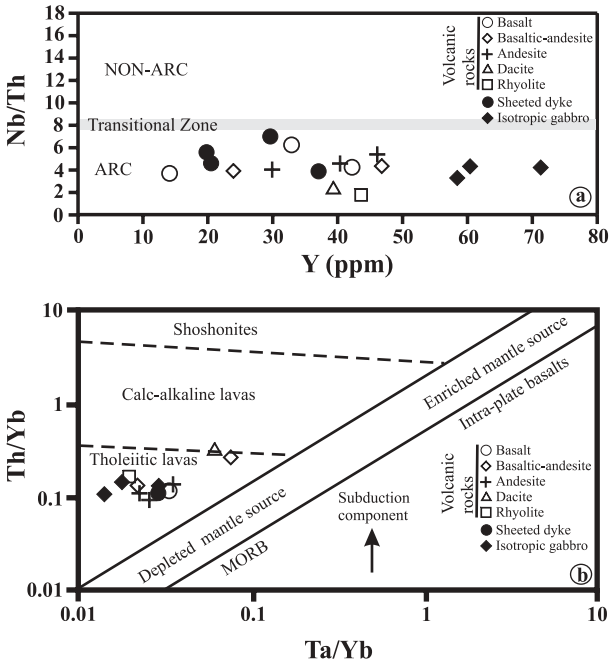


Figure 11. (a) Nb/Th v. Y diagram (after Jenner *et al*. 1991), showing the typically arc-like signature of the volcanic and subvolcanic rocks of the Göksun ophiolite. (b) Ta/Yb v. Th/Yb diagram (Pearce, 1982) for the volcanic and plutonic rocks of the Göksun ophiolite.

ophiolite was metamorphosed to amphibolite facies (Yazgan & Chessex, 1991) but still possesses a coherent ophiolite stratigraphy (Beyarslan & Bingöl, 2000). The unmetamorphosed Guleman and Ispendere ophiolites show a complete ophiolite pseudostratigraphy, from ultramafic rocks underlain tectonically by a metamorphic sole to volcanic rocks. Although the ophiolitic bodies have distinct features in terms of metamorphic grade, geographic distribution and absence/presence of sheeted dyke complexes, they are all thought to have originated as a single vast Late Cretaceous thrust sheet that was dispersed between the metamorphic massifs during the ongoing orogeny between Late Cretaceous and Late Miocene times (Şengör & Yılmaz, 1981; Yılmaz, Yiğitbaş & Genç, 1993; Beyarslan & Bingöl, 2000; Robertson, 2002). High-grade metamorphic sole rocks are observed in the Doğanşehir (Malatya) region in tectonic contact with overlying ophiolitic units; they display inverted metamorphic zonation from pyroxene–granulite facies to epidote–amphibolite facies. This metamorphic sole is thought to be the equivalent of the Berit metaophiolite (Perinçek & Kozlu, 1984; Genç, Yiğitbaş & Yılmaz, 1993) further to the southwest in the Göksun–Afşin (Kahramanmaraş) region. K–Ar isotopic age determination on the amphibole from the amphibolite facies yielded an age of 90 ± 7 Ma. Geochemically, seamounts, oceanic crust and sea-floor sediments entering the subduction zone were fragmented and accreted to the base of the hanging wall to form the metamorphic sole (Parlak *et al*. 2002). The volcanic–sedimentary unit, the Maden Group, contains a volcanic and sedimentary rock sequence of Middle Eocene age, possibly representing a short-lived back-arc basin (Yılmaz, Yiğitbaş & Genç, 1993; Yiğitbaş & Yılmaz, 1996) or pull-apart basin (Aktaş & Robertson, 1984). This indicates that the southerly Neotethyan oceanic basin remained open and subduction–accretion continued in southeastern Turkey into Tertiary times. All the tectonic units (Malatya–Keban platform, ophiolites and metamorphic sole) were intruded by a syn-collisional granitoids (~ 85 Ma) in the region (Parlak *et al*. 2001, 2002).

Several alternative tectonic models for the southeast Anatolian ophiolites have been suggested. The first is that all of the ophiolites were rooted to the northern

https://doi.org/10.1017/S0016756804009458 Published online by Cambridge University Press

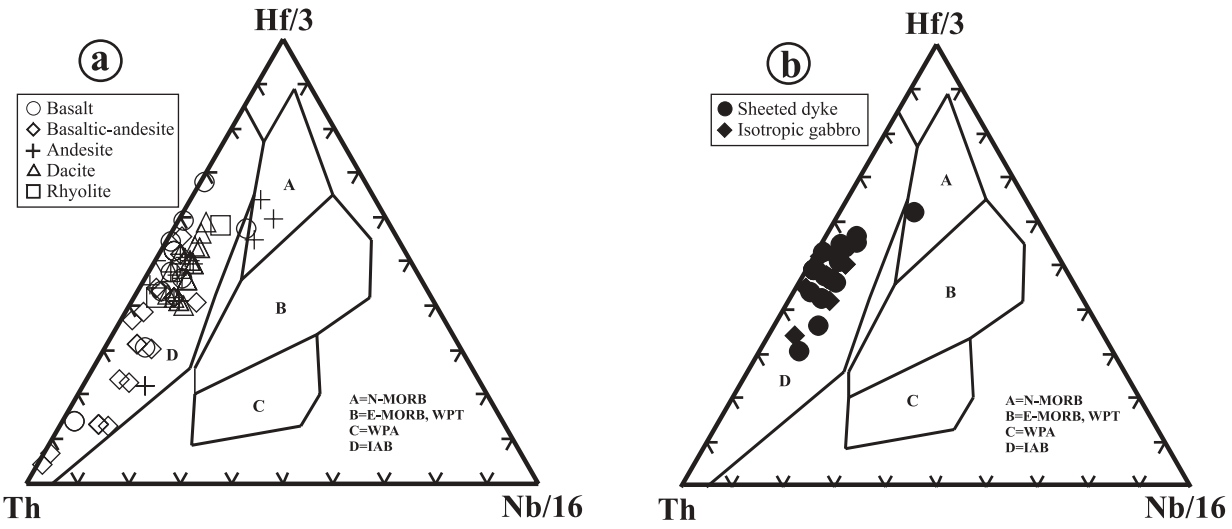


Figure 12. Tectonomagmatic discrimination diagrams for the volcanic rocks (a), sheeted dykes and isotropic gabbros (b) of the Göksun ophiolite (after Wood, 1980). N-MORB – Normal Mid-Ocean Ridge Basalt, E-MORB – Enriched Mid-Ocean Ridge Basalt, WPT – Within Plate Tholeiite, WPA – Within Plate Alkali, IAB – Island Arc Basalt.

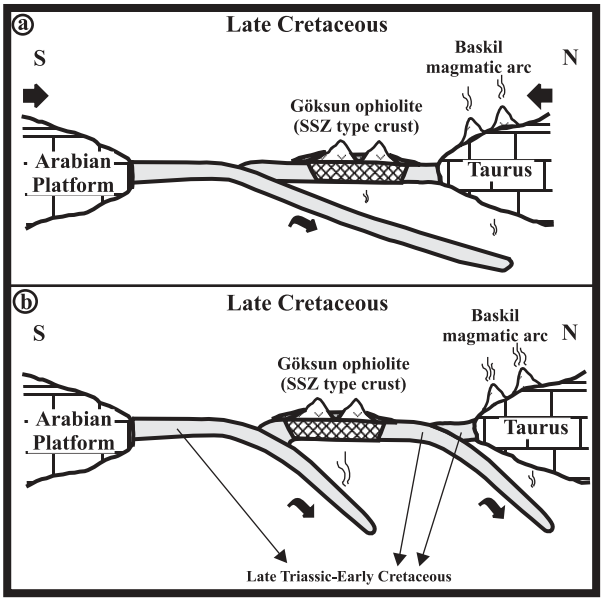


Figure 13. Alternative tectonic models ((a) single and (b) double subduction) for the formation of the Göksun ophiolite and Baskil magmatic arc in southeast Anatolia.

Neotethyan ocean (Ricou, Marcoux & Whitechurch, 1984). In this case, it is difficult to explain the tectonic position of the Keban platform as a passive margin in the south, intruded by the calc-alkaline arc type intrusive/extrusive rocks of the Baskil magmatics. The second model was put forward by Hall (1976), Aktaş & Robertson (1984, 1990), Yılmaz (1993) and Yılmaz, Yiğitbaş & Genç (1993). They propose a single subduction zone in a southern Neotethyan ocean, away from the continental margin on the oceanic side to the south, dipping to the north beneath the Tauride (Keban) platform (Fig. 13a). This single N-dipping subduction zone generated the ophiolites (Göksun, İspendere, Kömürhan, Guleman, etc.) above the intraoceanic subduction to the south as well as the Baskil magmatics on the active continental margin (Keban platform) to the north (Fig. 13a). Since the Göksun and other ophiolites (Kömürhan, İspendere and Guleman) represent well-developed oceanic crust generated during the inferred mature stage of the suprasubduction zone life cycle (Shervais, 2001), and the well-developed Baskil arc has a large volume of intrusive rocks cutting the Keban platform, it is unlikely that a single subduction would be sufficient to cause two well-developed tectonomagmatic events in the region. The third model, which is favoured in this paper, was proposed by Robertson (1998, 2000, 2002) and is shown in Figure 13b. This model requires two subduction zones, the first one beneath the Malatya–Keban platform generating the Baskil magmatic arc, and the second one on the oceanic side generating the Göksun and other ophiolites (Kömürhan, İspendere and Guleman) in a suprasubduction zone environment. Available cooling ages from the Baskil arc plutonics are 85 and 76 Ma, indicating that this partly post-dates the timing of the genesis of the suprasubduction zone ophiolites (~90 Ma). This evidence favours the 'double subduction zone model' since the 'single suprasubduction zone roll-back model' would imply abandonment of the arc prior to the genesis of supra-subduction zone-type ophiolites (Robertson, 2002). The significant subduction–accretion that took place is well constrained to the Early Tertiary. Therefore the double subduction model seems to be more favourable. The metamorphic sole rocks beneath the Göksun ophiolite were formed at the time of intraoceanic subduction. The high-grade metamorphic soles beneath the Göksun ophiolite would require a hot peridotite body (1000 °C) in addition to shear heating to be able to generate a granulite facies metamorphism during the

https://doi.org/10.1017/S0016756804009458 Published online by Cambridge University Press

intraoceanic thrusting (Spray, 1984). Granites that cut both the ophiolite and Malatya–Keban platform formed by partial melting of crustal rocks during prolonged subduction and thrusting of oceanic crust with the Andean type active margin (Parlak *et al*. 2001, 2002).

It is well known that the Late Cretaceous eastern Mediterranean ophiolites are different from the Jurassic western ophiolites of the Alps in terms of tectonic setting (Pearce, Lippard & Roberts, 1984) and the nature of the mantle tectonites (Nicolas, 1989). The Göksun ophiolite, one of the Late Cretaceous Neotethyan fragments in southern Turkey along the Alpine–Himalayan orogenic system, consists of well-preserved ophiolite pseudostratigraphy from bottom to top. The extrusive rocks (including basic, intermediate and acidic lavas) of the Göksun ophiolite show close similarity to the extrusive rocks of ophiolites in the eastern Mediterranean region.

## 7. Conclusions

The Göksun ophiolite was formed in a suprasubduction zone tectonic setting between the Arabian platform to the south and the Malatya–Keban platform to the north during Late Cretaceous times in southeast Anatolia. The suprasubduction zone tectonic setting includes island arcs, forearc and backarc basins for the generation of oceanic crust (ophiolite). Based on the field (arc-related volcanosedimentary units), petrographical (wide spectrum of rock units in volcanic rocks-basalt to rhyolite, highly evolved plutonic rocks such as diorite, Q-diorite and plagiogranite) and geochemical (flat-REE pattern, Nb depletion) data, the Göksun ophiolite is a good example of the island arc setting.

For the first time, an ophiolitic body formed in an island arc setting is studied geochemically in detail in Turkey. This particular ophiolite represents the mature stage of the suprasubduction zone life cycle based on the definition of Shervais (2001). There are number of ophiolites in the world which came to maturity. In order to preserve this stage of maturity, the ocean basin being subducted must be large enough to complete the first two stages (Shervais, 2001). The southern branch of the Neotethyan ocean in Turkey was the largest strand remaining open until the Late Cretaceous and this ocean reached its largest spread at the end of Early Cretaceous (Şengör & Yılmaz, 1981). Therefore, the southern branch of Neotethys was large enough for oceanic crust generation in a mature stage of a suprasubduction zone environment in southeast Anatolia.

Previously, this ophiolite body was interpreted as a complex that comprises a MOR-type oceanic crust formed during the opening stage of the Neotethyan ocean between Late Triassic and Late Cretaceous times, and a volcanic arc unit formed during the closure stage of the Neotethyan ocean in Late Cretaceous times. The geochemical data based on the immobile trace elements (including the rare earths) and the field evidence suggest that all the units (volcanic and plutonic rocks) were formed during the closure stage of the southern branch of the Neotethys in the Late Cretaceous period.

**Acknowledgements.** This research was supported by TÜBİTAK (Scientific and Technical Research Council of Turkey, Project Number: YDABÇAG-199Y011) and the Çukurova University Scientific Research Projects (MMF2002BAP41). We are indebted to Fabio Capponi (University of Geneva) and Jean Claude Lavanchy (University of Lausanne) for performing major and trace element analyses. Utku Bağcı, Tamer Rızaoğlu and Alaiddin Bolat are thanked for their field assistance. Yıldırım Dilek and John Shervais are thanked for their helpful reviews that improved the manuscript. Grateful thanks are due to Alastair Robertson for his suggestions on the revised version. Jane Holland and David Pyle are thanked for editorial handling. OP also acknowledges the financial support from the Turkish Academy of Sciences, in the frame of the Young Scientist Award Program (TÜBA-GEBİP).

## References

AKTAŞ, G. & ROBERTSON, A. H. F. 1984. The Maden complex, SE Turkey: evolution of a Neotethyan continental margin. In *The Geological Evolution of the eastern Mediterranean* (eds J. E. Dixon and A. H. F. Robertson), pp. 375–402. Geological Society of London, Special Publication no. 17.

AKTAŞ, G. & ROBERTSON, A. H. F. 1990. Tectonic evolution of the Tethys suture zone in S. E. Turkey: evolution evidence from the petrology and geochemistry of Late Cretaceous and Middle Eocene extrusives. In *Ophiolites – oceanic crustal analogues: Proceedings of Troodos ophiolite symposium – 1987* (eds J. Malpas, E. Moores, A. Panayiotou and C. Xenophontos), pp. 311–29. Geological Survey, Cyprus.

ALABASTER, T., PEARCE, J. A. & MALPAS, J. 1982. The volcanic stratigraphy and petrogenesis of the Oman ophiolite complex. *Contributions to Mineralogy and Petrology* **81**, 168–83.

AL-RIYAMI, K., ROBERTSON, A., DIXON, J. & XENOPHONTOS, C. 2002. Origin and emplacement of the Late Cretaceous Baer–Bassit ophiolite and its metamorphic sole in NW Syria. *Lithos* **65**, 225–60.

ARCULUS, R. J. & POWELL, R. 1986. Source component mixing in the regions of arc magma generation. *Journal of Geophysical Research* **19**, 5913–26.

BECCALUVA, L., COLTORI, M., PREMTI, I., SACCANI, E., SIENA, F. & ZEDA, O. 1994. Mid-ocean ridge and suprasubduction zone ophiolites in Albania. *Ofioliti* **19**, 77–9.

BEYARSLAN, M. & BİNGÖL, A. F. 2000. Petrology of a suprasubduction zone ophiolite (Elazığ, Turkey). *Canadian Journal of Earth Sciences* **37**, 1411–24.

BORTOLOTTI, V., KODRA, A., MARRONI, M., MUSTAFA, F., PANDOLFI, L., PRINCIPI, G. & SACCANI, E. 1996. Geology and petrology of ophiolitic sequences in the Mirdita region (Northern Albania). *Ofioliti* **21**, 3–20.

CAPEDRI, S., VENTURELLI, G., BOCCHI, G., DOSTAL, J., GARURI, G. & ROSSI, A. 1980. The geochemistry and petrogenesis of an ophiolite sequence from Pindos, Greece. *Contributions to Mineralogy and Petrology* **74**, 189–200.

DİLEK, Y. & DELALOYE, M. 1992. Structure of the Kızıldağ ophiolite, a slow-spread Cretaceous ridge segment north of the Arabian promontory. *Geology* **20**, 19–22.

DİLEK, Y. & MOORES, E. 1990. Regional tectonics of the eastern Mediterranean ophiolites. In *Ophiolites – oceanic crustal analogues: Proceedings of Troodos ophiolite symposium – 1987* (eds J. Malpas, E. Moores, A. Panayiotou and C. Xenophontos), pp. 295–309. Geological Survey, Cyprus.

DİLEK, Y. & THY, P. 1998. Structure, petrology and seafloor spreading tectonics of the Kizildag ophiolite, Turkey. In *Modern Ocean Floor Processes and the Geological Record* (eds R. A. Mills and K. Harrison), pp. 43–69. Geological Society of London, Special Publication no. 148.

DİLEK, Y., THY, P., HACKER, B. & GRUNDVIG, S. 1999. Structure and petrology of Tauride ophiolites and mafic dyke intrusions (Turkey): implications for the Neotethyan ocean. *Geological Society of America Bulletin* **111**, 1192–1216.

DUBERTRET, L. 1955. Géologie des roches vertes du nord-ouest de la Syrie et du Hatay (Turquie). *Notes Mémoire Moyen-Orient* **6**, 227 pp.

DUNNE, L. A. & HEMPTON, M. R. 1984. Strike-slipe basin sedimentation at Lake Hazar (Eastern Taurus Mountains). In *Proceedings of International Symposium on the Geology of Taurus Belt* (eds O. Tekeli and M. C. Göncüoğlu), pp. 229–35. MTA-Ankara, Turkey.

ELTHON, D. 1991. Geochemical evidence for formation of the Bay of Islands ophiolite above a subduction zone. *Nature* **354**, 140–3.

FLOYD, P. A. & WINCHESTER, J. A. 1978. Identification and discrimination of altered and metamorphosed volcanic rocks using immobile elements. *Chemical Geology* **21**, 291–306.

FLOYD, P. A. & WINCHESTER, J. A. 1975. Magma type and tectonic setting discrimination using immobile elements. *Earth and Planetary Science Letters* **27**, 211–18.

GENÇ, S. C., YİĞİTBAŞ, E. & YILMAZ, Y. 1993. Berit metaofiyolitinin jeolojisi. In *Proceedings of Suat Erk Geology Symposium* (ed. N. Kazancı), pp. 37–52. Ankara University Geology Department.

HALL, R. 1976. Ophiolite emplacement and the evolution of the Taurus suture zone, south-east Turkey. *Geological Society of America Bulletin* **87**, 1078–88.

HÉBERT, R. & LAURENT, R. 1990. Mineral chemistry of the plutonic section of the Troodos ophiolite: New constraints for genesis of arc-related ophiolites. In *Ophiolites – oceanic crustal analogues: Proceedings of Troodos ophiolite symposium – 1987* (eds J. Malpas, E. Moores, A. Panayiotou and C. Xenophontos), pp. 149–63. Geological Survey, Cyprus.

HÖCK, V., KOLLER, F., MEISEL, T., ONUZI, K. & KNERINGER, E. 2002. The Jurassic south Albanian ophiolites: MOR- vs SSZ-type ophiolites. Lithos **65**, 143–64.

HUMPHRIS, S. E. & THOMPSON, G. 1978. Trace element mobility during hydrothermal alteration of oceanic basalts. *Geochimica et Cosmochimica Acta* **42**, 127–36.

IRVINE, T. N. & BARAGAR, W. R. A. 1971. A guide to the chemical classification of the common volcanic rocks. *Canadian Journal of Earth Sciences* **8**, 523–48.

JAKES, P. & GILL, J. 1970. Rare earth elements and the island arc tholeiitic series. *Earth and Planetary Science Letters* **9**, 17–28.

JENNER, G. A., DUNNING, G. R., MALPAS, J., BROWN, M. & BRACE, T. 1991. Bay of Islands and Little Port complexes, revisited: age, geochemical and isotopic evidence confirm suprasubduction-zone origin. *Canadian Journal of Earth Sciences* **28**, 1635–52.

JONES, G., ROBERTSON, A. H. F. & CANN, J. R. 1991. Genesis and emplacement of the suprasubduction zone Pindos ophiolite, northwestern Greece. In *Ophiolite genesis and evolution of the oceanic lithosphere* (eds T. J. Peters, A. Nicolas and R. G. Coleman), pp. 771–9. Dordrecht: Kluwer Academic Publishing.

JUTEAU, T. 1980. Ophiolites of Turkey. *Ofioliti* **2**, 199–238.

KARIG, D. E. & KOZLU, H. 1990. Late Paleogene–Neogene evolution of the triple junction near Maraş, south-central Turkey. *Journal of the Geological Society, London* **147**, 1023–34.

KETİN, I. 1983. Türkiye Jeolojisine genel bir bakis. *ITÜ Kütüphanesi* **1259**, 595 pp.

KOEPKE, J., SEIDEL, E. & KREUZER, H. 2002. Ophiolites on the southern Aegean Islands, Crete, Karpathos and Rhodes. *Lithos* **65**, 183–203.

LYTWYN, J. N. & CASEY, J. F. 1995. The geochemistry of postkinematic mafic dyke swarms and subophiolitic metabasites, Pozantı–Karsantı ophiolite, Turkey: Evidence for ridge subduction. *Geological Society of America Bulletin* **107**, 830–50.

LYTWYN, J. N. & CASEY, J. F. 1993. The geochemistry and petrogenesis of volcanic rocks and sheeted dykes from the Hatay (Kızıldağ) ophiolite, southern Turkey: possible formation with the Troodos ophiolite, Cyprus, along fore-arc spreading centers. *Tectonophysics* **223**, 237–72.

NICOLAS, A. 1989. *Structures of ophiolites and dynamics of oceanic lithosphere*. Dordrecht: Kluwer Academic Publishers, 366 pp.

PAMIC, J., TOMLJENOVIC, B. & BALEN, D. 2002. Geodynamic and petrogenetic evolution of Alpine ophiolites from the central and NW Dinarides: an overview. *Lithos* **65**, 113–42.

PARLAK, O. 1996. Geochemistry and geochronology of the Mersin ophiolite within the eastern Mediterranean tectonic frame. *Terre et Environnement* **6**, published Ph.D. thesis, University of Geneva, 242 pp.

PARLAK, O., DELALOYE, M. & BİNGÖL, E. 1995. Geochemistry of the volcanic rocks in the Mersin ophiolite (southern Turkey) and their tectonic significance in the eastern Mediterranean *geology*. In *International Earth Science Colloquium on the Aegean region-IESCA 1995* (eds Ö. Piskin, M. Ergün, M. Y. Savasçin and G. Tarcan), pp. 441–63. Dokuz Eylül University, Izmir, Turkey.

PARLAK, O., DELALOYE, M. & BİNGÖL, E. 1996. Mineral chemistry of ultramafic and mafic cumulates as an indicator of the arc-related origin of the Mersin ophiolite (southern Turkey). *Geologische Rundschau* **85**, 647–61.

PARLAK, O., HÖCK, V. & DELALOYE, M. 2000. Suprasubduction zone origin of the Pozantı–Karsantı ophiolite (southern Turkey) deduced from whole-rock and mineral chemistry of the gabbroic cumulates. In *Tectonics and magmatism in Turkey and the surrounding area* (eds E. Bozkurt, J. A. Winchester and J. D. A. Piper), pp. 219–34. Geological Society of London, Special Publication no. 173.

PARLAK, O., HÖCK, V. & DELALOYE, M. 2002. The suprasubduction Pozantı–Karsantı ophiolite, southern Turkey: evidence for high-pressure crystal fractionation of ultramafic cumulates. *Lithos* **65**, 205–24.

PARLAK, O., KOZLU, H., DELALOYE, M. & HÖCK, V. 2001. Tectonic setting of the Yüksekova ophiolite and its relation to the Baskil magmatic arc within the southeast Anatolian orogeny. In *4th International Turkish Geology Symposium (ITGS-IV), 24–28 September 2001, Çukurova University, Adana -Turkey*, p. 233.

PARLAK, O., ÖNAL, A., HÖCK, V., KÜRÜM, S., DELALOYE, M., BAĞCI, U. & RIZAOĞLU, T. 2002. Inverted metamorphic zonation beneath the Yüksekova ophiolite in SE Anatolia. In *1st International symposium of the faculty of Mines (ITU) on Earth Science and Engineering, 16–18 May* 2002, *Istanbul-Turkey*, p. 133.

PEARCE, J. A. 1983. Role of the subcontinental lithosphere in magma genesis at active continental margins. In *Continental basalts and mantle xenoliths* (eds C. J. Hawkesworth and M. J. Norry), pp. 230–49. Cheshire: Shiva Publishing.

PEARCE, J. A. 1982. Trace element characteristics of lavas from destructive plate boundaries. In *Andesites* (ed. R. S. Thorpe), pp. 525–48. New York: Wiley.

PEARCE, J. A. & CANN, J. R. 1973. Tectonic setting of basaltic volcanic rocks determined using trace element analysis. *Earth and Planetary Science Letters* **19**, 290–300.

PEARCE, J. A., LIPPARD, S. J. & ROBERTS, S. 1984. Characteristics and tectonic significance of suprasubduction zone ophiolites. In *Marginal basin geology* (eds B. P. Kokelaar and M. F. Howells), pp. 77–94. Geological Society of London, Special Publication no. 16.

PEARCE, J. A. & NORRY, M. J. 1979. Petrogenetic implications of Ti, Zr, Y and Nb variations in volcanic rocks. *Contributions to Mineralogy and Petrology* **69**, 33–47.

PERİNÇEK, D. & KOZLU, H. 1984. Stratigraphy and structural relations of the units in the Afşin-Elbistan-Doğanşehir region (Eastern Taurus). In *Proceedings of International Symposium on the Geology of Taurus Belt* (eds O. Tekeli and M. C. Göncüoğlu), pp. 181–98. Ankara, Turkey.

RASSIOS, A., BECCALUVA, L., BORTOLOTTI, V. & MOORES, E. M. 1983. The Vourinos ophiolite complex. *Ofioliti* **8**, 275–92.

RICOU, L. E., MARCOUX, J. & WHITECHURCH, H. 1984. The Mesozoic organization of the Taurides: one or several oceanic basins. In *The Geological Evolution of the eastern Mediterranean* (eds J. E. Dixon and A. H. F. Robertson), pp. 349–60. Geological Society of London, Special Publication no. 17.

ROBERTSON, A. H. F. 2002. Overview of the genesis and emplacement of Mesozoic ophiolites in the Eastern Mediterranean Tethyan region. *Lithos* **65**, 1–67.

ROBERTSON, A. H. F. 2000. Mesozoic–Tertiary tectonic-sedimentary evolution of a south Tethyan oceanic basin and its margins in southern Turkey. In *Tectonics and magmatism in Turkey and the surrounding area* (eds E. Bozkurt, J. A. Winchester and J. D. A. Piper), pp. 97–138. Geological Society of London, Special Publication no. 173.

ROBERTSON, A. H. F. 1998. Mesozoic–Tertiary tectonic evolution of the easternmost Mediterranean area; integration of marine and land evidence. In *Proceedings of the Ocean Drilling Program, Scientific Results, vol. 160* (eds A. H. F. Robertson, K. C. Emeis, K. C. Richter and A. Camerlenghi), pp. 723–82. College Station, Texas.

ROBERTSON, A. H. F. & DIXON, J. E. 1984. Introduction: aspects of the geological evolution of the Eastern Mediterranean. In *The Geological Evolution of the Eastern Mediterranean* (J. E. Dixon and A. H. F. Robertson), pp. 1–74. Geological Society of London, Special Publication no. 17.

ROBERTSON, A. H. F. & SHALLO, M. 2000. Mesozoic–Tertiary tectonic evolution of Albania in its regional eastern Mediterranean context. *Tectonophysics* **316**, 197–214.

ROLLINSON, H. 1993. Using geochemical data: evaluation, presentation, interpretation. Longman Group, UK, 352 pp.

ŞENGÖR, A. M. C. & YILMAZ, Y. 1981. Tethyan evolution of Turkey: a plate tectonic approach. *Tectonophysics* **75**, 181–241.

SHALLO, M., KODRA, A. & Gjata, K. 1990. Geo tectonics of the Albanian ophiolites. In *Ophiolites – oceanic crustal analogues: Proceedings of Troodos ophiolite symposium – 1987* (eds J. Malpas, E. Moores, A. Panayiotou and C. Xenophontos), pp. 265–70. Geological Survey, Cyprus.

SHERVAIS, J. W. 2001. Birth, death and resurrection: The life cycle of suprasubduction zone ophiolites. *Geochemistry, Geophysics, Geosystems* **2**, 45 pp., 2000GC000080.

SMITH, A. G., HYNES, A. J., MENZIES, M., NISBET, E. G., PRICE, I., WELLAND, M. J. & FERRIERE, J. 1975. The stratigraphy of the Othris Mountains, Eastern Central Greece: a deformed Mesozoic continental margin sequence. *Eclogae Geologica Helvetica* **68**, 463–81.

SPRAY, J. G. 1984. Possible causes and consequences of upper mantle decoupling and ophiolite displacement. In *Ophiolites and oceanic lithosphere* (eds I. G. Gass, S. J. Lippard and A. W. Shelton), pp. 255–68. Oxford: Blackwell.

SUN, S. S. & MCDONOUGH, W. F. 1989. Chemical and isotopic systematics of oceanic basalts: implications for mantle composition and processes. In *Magmatism in the ocean basins* (eds A. D. Saunders and M. J. Norry), pp. 313–47. Geological Society of London, Special Publication no. 42.

THOMPSON, G. 1973. A geochemical study of the low temperature interaction of seawater and oceanic igneous rocks. *Transactions of American Geophysical Union* **54**, 1015–19.

THY, P. 1987. Petrogenetic implications of mineral crystallization trends of Troodos cumulates, Cyprus. *Geological Magazine* **124**, 1–11.

USTAÖMER, T. & ROBERTSON, A. H. F. 1997. Tectonic-sedimentary evolution of the north Tethyan margin in the Central Pontidesof northern Turkey. In *Regional and Petroleum Geology of the Black Sea and Surrounding Region* (ed. A. G. Robinson), pp. 255–90. American Association of Petroleum Geologists, Memoir no. 68.

WALLIN, E. T. & METCALF, R. V. 1998. Supra-subduction zone ophiolites formed in an extensional forearc: Trinity Terrane, Klamath Mountains, California. *Journal of Geology* **106**, 591–608.

WINCHESTER, J. A. & FLOYD, P. A. 1977. Geochemical discrimination of different magma series and their differentiation products using immobile elements. *Chemical Geology* **20**, 325–43.

WOOD, D. A. 1980. The application of a Th–Hf–Ta diagram to problems of tectonomagmatic classification and to establishing the nature of crustal contamination of basaltic lavas of the British Tertiary volcanic province. *Earth and Planetary Science Letters* **56**, 11–30.

WOOD, D. A., JORON, J. L. & TREUIL, M. 1979. A reappraisal of the use of trace elements to classify and discriminate between magma series erupted in different tectonic

settings. *Earth and Planetary Science Letters* **45**, 326–36.

YALINIZ, K. M., FLOYD, P. & GÖNCÜOĞLU, M. C. 1996. Supra-subduction zone ophiolites of Central Anatolia: geochemical evidence from the Sarikaraman ophiolite, Aksaray, Turkey. *Mineralogical Magazine* **60**, 697–710.

YALINIZ, K. M., FLOYD, P. & GÖNCÜOĞLU, M. C. 2000. Geochemistry of volcanic rocks from the Çiçekdag ophiolite, Central Anatolia, *Turkey*, and their inferred tectonic setting within the northern branch of the Neotethyan ocean. In *Tectonics and magmatism in Turkey and the surrounding area* (eds E. Bozkurt, J. A. Winchester and J. D. A. Piper), pp. 203–18. Geological Society of London, Special Publication no. 173.

YAZGAN, E. & CHESSEX, R. 1991. Geology and tectonic evolution of the southeastern Taurides in the region of Malatya. *Turkish Association of Petroleum Geologists* **3**, 1–42.

YILMAZ, Y. 1993. New Evidence and Model on The Evolution of The Southeast Anatolian Orogen. *Geological Society of America Bulletin* **105**, 251–71.

YILMAZ, Y. 1990. Allochthonous terranes in the Tethyan middle east: Anatolia and surrounding regions. *Royal Society of London Philosophical Transactions* **A331**, 611–24.

YILMAZ, Y., GÜRPINAR, O., KOZLU, H., GÜL, M. A., YİĞİTBAŞ, E., YILDIRIM, M., GENÇ, C. & KESKİN, M. 1987. Kahramanmaraş Kuzeyinin Jeolojisi (Andırın–Berit–Engizek–Nurhak–Binboğa Dağları). *Türkiye Petrolleri A. O. Rapor No.* 2028, Ankara, 218 pp.

YILMAZ, Y. & YİĞİTBAŞ, E. 1991. The different ophiolitic-metamorphic assemblages of SE Anatolia and their significance in the geological evolution of the region. *Proceedings of 8th Petroleum Congress of Turkey, Ankara, Turkey*, pp. 128–40. Turkish Association of Petroleum Geologists.

YILMAZ, Y., YİĞİTBAŞ, E. & GENÇ, Ş. C. 1993. Ophiolitic and Metamorphic Assemblages of Southeast Anatolia and their Significance in the Geological Evolution of the Orogenic Belt. *Tectonics* **12**, 1280–97.

YİĞİTBAŞ, E. & YILMAZ, Y. 1996. New evidence and solution to the Maden complex controversy of the southeast Anatolian orogenic belt (Turkey). *Geologische Rundschau* **85**, 250–63.

YOGODZINSKI, G. M., VOLYNETS, O. N., KOLOSKOV, A. V., SELIVERSTOV, N. I. & MATVENKOV, V. V. 1993. Magnesian andesites and the subduction component in strongly calc-alkaline series at Piip volcano, far western Aleutians. *Journal of Petrology* **35**, 163–204.